

SEQUENTIAL GROWTH FACTOR DELIVERY FROM COMPLEXED
MICROSPHERES FOR BONE TISSUE ENGINEERING

A THESIS SUBMITTED TO
THE GRADUATE SCHOOL OF NATURAL AND APPLIED SCIENCES
OF
MIDDLE EAST TECHNICAL UNIVERSITY

BY

FİTNAT BUKET BAŞMANAV

IN PARTIAL FULFILLMENT OF THE REQUIREMENTS
FOR
THE DEGREE OF MASTER OF SCIENCE
IN
BIOTECHNOLOGY

SEPTEMBER 2007

Approval of the thesis:

**SEQUENTIAL GROWTH FACTOR DELIVERY FROM COMPLEXED
MICROSPHERES FOR BONE TISSUE ENGINEERING**

submitted by **FİTNAT BUKET BAŞMANAV** in partial fulfillment of the requirements for the degree of **Master of Science in Biotechnology, Middle East Technical University** by,

Prof. Dr. Canan Özgen

Dean, Graduate School of **Natural and Applied Sciences**

Prof. Dr. Fatih Yıldız

Head of Department, **Biotechnology**

Prof. Dr. Vasıf Hasırcı

Supervisor, **Biological Sciences Dept., METU**

Assoc. Prof. Dr. Gamze Torun Köse

Co-Supervisor, **Genetics and Bioengineering Dept., Yeditepe University**

Examining Committee Members:

Prof. Dr. Aykut Özkul

Faculty of Veterinary Medicine, Ankara University

Prof. Dr. Vasıf Hasırcı

Biological Sciences Dept., METU

Prof. Dr. Faruk Bozođlu

Food Engineering Dept., METU

Prof. Dr. Hüseyin Avni Öktem

Biological Sciences Dept., METU

Assist. Prof. Dr. Ayşegül Gözen

Biological Sciences Dept., METU

Date: _____

I hereby declare that all information in this document has been obtained and presented in accordance with academic rules and ethical conduct. I also declare that, as required by these rules and conduct, I have fully cited and referenced all material and results that are not original to this work.

Name, Last name : Fitnat Buket BAŞMANAV

Signature :

ABSTRACT

SEQUENTIAL GROWTH FACTOR DELIVERY FROM COMPLEXED MICROSPHERES FOR BONE TISSUE ENGINEERING

Başmanav, Fitnat Buket

M.S., Department of Biotechnology

Supervisor : Prof. Dr. Vasif Hasırcı

Co-Supervisor : Assoc. Prof. Dr. Gamze Torun Köse

September 2007, 93 pages

Complexed microspheres of poly(4-vinyl pyridine) (P₄VN) and alginic acid were prepared by internal gelation method and subsequent freeze drying.

The 4% and 10% microspheres were loaded with Bone Morphogenetic Protein-2 (BMP-2) and Bone Morphogenetic Protein-7 (BMP-7), respectively for *in vitro* studies and were entrapped in PLGA foams. Foams containing only 4%, BMP-2 microspheres, only 10%, BMP-7 microspheres and both populations were prepared. Control samples of each group were prepared with drug free microspheres. Bone marrow derived stem cells from rat femur and tibia isolated by a surgical operation, were seeded onto foams.

Proliferation of cells on foams containing both microsphere populations was higher at all time points regardless of the presence of BMPs. This was attributed to different porosity characteristics. Proliferation was higher at all times in control samples in comparison to their positive samples for all groups, suggesting proliferation attenuation related enhancement in osteogenic activity due to BMP supply.

Alkaline phosphatase (ALP) activities were lower at all time points for foams containing both microsphere populations regardless of BMP presence. This was attributed to different physical characteristics of foams confirmed by the inverse correlation between proliferation and osteogenic differentiation. Total and specific ALP activity results demonstrated the significant positive influence of all BMP containing types in enhancing osteogenic differentiation. Best results were obtained with co-administration of sequential delivery performing 4% and 10% microspheres loaded with BMP-2 and BMP-7, respectively.

Keywords: Bone Tissue Engineering, Complex Microspheres, Bone Morphogenetic Proteins, Sequential Delivery

ÖZ

KEMİK DOKU MÜHENDİSLİĞİ AMACIYLA MİKROKÜRELERDEN ARDIŞIK BÜYÜME FAKTÖRÜ SALIMI

Başmanav, Fitnat Buket

Yüksek Lisans, Biyoteknoloji ABD

Tez Yöneticisi : Prof. Dr. Vasıf Hasırcı

Ortak Tez Yöneticisi : Doç. Dr. Gamze Torun Köse

Eylül 2007, 93 sayfa

Bu çalışmada, poli(4-vinilpiridin) ve aljinik asitten oluşan mikroküreler iç jelleşme yöntemiyle hazırlanmış ve daha sonra vakum altında kurutulmuştur.

Hücre çalışmaları için %4'lük ve %10'luk küreler sırasıyla kemik morfogenezini tetikleyici protein-2 (BMP-2) ve kemik morfogenezini tetikleyici protein-7 (BMP-7) ile yüklenmiş ve PLGA hücre taşıyıcılar içine hapsedilmiştir. Yalnız %4'lük BMP-2 kürelerini barındıran, yalnız %10'luk BMP-7 kürelerini barındıran ve her iki küre grubunu da barındıran hücre taşıyıcılar hazırlanmıştır. Kontrol örnekleri olarak her bir grup için BMP içermeyen küreleri barındıran hücre taşıyıcılar hazırlanmıştır. Hücre taşıyıcıların üzerine sıçan kemik iliğinden izole edilen kök hücreler ekilmiştir.

Tüm zamanlarda hücre büyümesinin BMP varlığından bağımsız olarak, her iki küre grubunu da barındıran taşıyıcılar üzerinde en yüksek olduğu belirlenmiştir. Bu bulgu, bu tip taşıyıcıların gözenek dağılımının diğer taşıyıcılarındakinden belirgin biçimde farklı olmasına bağlanmıştır. Grupların tamamında, tüm zamanlarda hücre büyümesinin BMP yüklü olmayan kontrol örneklerinde daha yüksek olduğu gözlemlenmiştir. Bu durumun, BMP varlığı ile artan osteogenetik aktiviteye bağlı olabileceği sonucuna varılmıştır.

ALP aktivitesinin BMP varlığından bağımsız olarak tüm zamanlarda iki popülasyonu da barındıran taşıyıcılarda en düşük olduğu gözlemlenmiştir. Bu bulgu osteogenez ve hücre büyümesi arasında ters bir ilişki olduğunu ve taşıyıcıların fiziksel özelliklerinin osteogenez üzerindeki etkisini göstermiştir. Toplam ve hücre başına düşen ALP aktivite sonuçları, bütün gruplarda BMP varlığının osteogenezi arttırıcı etkisini belirgin biçimde ortaya koymuştur. En büyük etki ise %4'lük BMP-2 ve %10'luk BMP-7 yüklü kürelerin beraber bulunduğu grup için gözlemlenmiştir.

Anahtar kelimeler: Kemik Doku Mühendisliği, Mikroküre, Ardışık Salım, Kemik Morfogenezi tetikleyici protein

To my dearest parents Seçil and Erman Başmanav

ACKNOWLEDGEMENTS

I express my most sincere gratitude to my supervisor Prof. Dr. Vasif Hasirci, for his continuous moral support, scientific guidance and help throughout this study and for being the best supervisor ever.

I also like to thank Assoc. Prof. Dr. Gamze Torun Köse for her contributions to this study as my co-supervisor.

I express my very special thanks to Pinar Zorlutuna and Pinar Yilgör for their precious help and support during this study. I also thank my other labmates, Engin Vrana, Halime Kenar, Arda Büyüksungur, Albana Ndreu, Nihan Öztürk, Deniz Yücel, Erkin Aydın, Banu Bayyurt and Beste Kinikoğlu, Hayriye Özçelik; they have all contributed to this study.

I express my special thanks to Zeynel Akın, Melis Or, Taylan Özerkan and Aysel Kızıltay for their valuable help and moral support throughout this study.

I acknowledge EU FP6 "BioPolySurf" Project and METU BAP-2007-07-02-00-01 through which the research was funded and TUBITAK TBAG Project-105T508 for personal funding.

I thank METU Central Laboratory for analyses done in their facilities.

At last but definitely not the least, I express my most sincere gratitudes to Seçil Başmanav, Erman Başmanav, Nilüfer Afşar, Oğulcan Başmanav and every other single member of my wonderful family for always being next to me with love, support, understanding and caring. Finally, I express my very special thanks to my dearest grandmother Fitnat Başmanav.

TABLE OF CONTENTS

ABSTRACT	iv
ÖZ.....	vi
ACKNOWLEDGEMENTS	ix
TABLE OF CONTENTS	x
LIST OF TABLES	xiii
LIST OF FIGURES	xiv
LIST OF ABBREVIATIONS.....	xvi
CHAPTERS	1
1 INTRODUCTION	1
1.1 Tissue Engineering	1
1.1.1 Bone Tissue Engineering	2
1.2 Scaffolds in Bone Tissue Engineering	4
1.2.1 Natural Polymers as Scaffold Materials	5
1.2.2 Synthetic Polymers as Scaffold Materials	7
1.2.3 Ceramics and Composites as Scaffold Materials	9
1.3 Stem Cell Based Bone Tissue Engineering.....	11
1.4 Bioactive Agents in Bone Tissue Engineering	14
1.4.1 BMPs in Bone Tissue Engineering	16
1.4.1.1 BMPs in Osteogenic Differentiation of MSCs	18
1.5 Delivery of Bioactive Agents in Bone Tissue Engineering	18
1.5.1 Delivery of Multiple Bioactive Agents.....	19
1.5.2 Incorporation of Bioactive Agents into Scaffolds	21
1.5.2.1 Direct Incorporation of Bioactive Agents into Scaffolds	21
1.5.2.2 Micro/Nanoparticle Mediated Delivery from Scaffolds.....	22
1.6 Scope of the Study.....	24

2 MATERIALS AND METHODS	25
2.1 Materials	25
2.2 Methods	26
2.2.1 Preparation of P ₄ VN-Alginate-BSA Microspheres.....	26
2.2.2 Characterization of the Microsphere Populations	27
2.2.2.1 Stereomicroscopy of Microspheres.....	27
2.2.2.2 Scanning Electron Microscopy of Microspheres	27
2.2.3 Determination of Encapsulation Efficiency	27
2.2.4 <i>In situ</i> Release Studies	28
2.2.5 Preparation of PLGA Foams with Entrapped Microspheres.....	28
2.2.6 Characterization of Foams.....	29
2.2.6.1 Stereomicroscopy	29
2.2.6.2 Scanning Electron Microscopy	29
2.2.6.3 Pore Size Distribution Analysis	29
2.2.7 <i>In vitro</i> Studies.....	29
2.2.7.1 Isolation of Rat Bone Marrow Stem Cells	30
2.2.7.2 Culture of Bone Marrow Stem Cells.....	31
2.2.7.3 Cell Seeding on Foams.....	32
2.2.7.4 Cell Proliferation Assay	32
2.2.7.4.1 Alamar Blue Optimization for BMSc.....	32
2.2.7.4.2 Cell Proliferation	33
2.2.7.5 Determination of Cell Differentiation by ALP Assay	34
2.2.7.6 Phalloidin Staining	35
2.2.7.7 SEM images of Cell Cultured Foams	35
3 RESULTS AND DISCUSSION	36
3.1 <i>In situ</i> Release Profiles of P ₄ VN-BSA-Alginate Microspheres	36
3.1.1 Influence of Polymer Concentration on Release Behavior	36
3.1.2 Influence of Crosslinking Duration on Release Behavior	40
3.1.3 Influence of Crosslinking Temperature on Release Behavior	41
3.2 BSA Entrapment Efficiency of P ₄ VN-Alginate Microspheres.....	43
3.2.1 Influence of Polymer Concentration on Entrapment Efficiency	43
3.2.2 Influence of Crosslinking Duration on Entrapment Efficiency.....	45
3.2.3 Influence of Crosslinking Temperature on Entrapment Efficiency .	47

3.3 Microscopy of Microsphere Populations	48
3.3.1 Stereomicroscopy	48
3.3.2 Scanning Electron Microscopy	49
3.4. Microscopy of Foams	50
3.4.1 Stereomicroscopy	50
3.4.2 Scanning Electron Microscopy	52
3.5. Pore Size Distribution Analysis of Foams with Microspheres.....	53
3.6 In vitro Studies.....	55
3.6.1 Cell Proliferation	55
3.6.2 ALP Activity.....	57
3.6.3 Specific ALP Activity	61
3.6.4 Phalloidin Staining.....	64
3.6.5 Scanning Electron Microscopy	66
4 CONCLUSION	68
REFERENCES	71
APPENDIX A.....	90
APPENDIX B.....	91
APPENDIX C.....	92
APPENDIX D	93

LIST OF TABLES

Table 1. Microsphere samples and their preparation conditions.....	26
Table 2. Foam samples and their compositions.....	28
Table 3. Microsphere loaded foams used in <i>in vitro</i> studies	30
Table 4. Kinetic analysis of release from microspheres of different polymer concentrations	39
Table 5. Kinetic analysis of release from microspheres with different crosslinking durations.....	41
Table 6. Kinetic analysis of release from microspheres with different crosslinking temperatures	43
Table 7. Effect of polymer concentration on entrapment efficiency	44
Table 8. Effect of polymer concentration and crosslinking duration on entrapment efficiency.....	45
Table 9. Effect of crosslinking temperature on entrapment efficiency	47

LIST OF FIGURES

Figure 1. Schematic representation of the system designed.	24
Figure 2. Influence of polymer concentration on BSA release from 4%, 6%, 8% and 10% microspheres.	36
Figure 3. Kinetic analysis of 4% microspheres in accordance with Higuchi release model.	38
Figure 4. Influence of crosslinking duration on BSA release from 4% and 10% microspheres.	40
Figure 5. Influence of crosslinking temperature on BSA release from 4% and 10% microspheres.	42
Figure 6. Stereomicrographs of microspheres.	48
Figure 7. SEM images of microspheres.	50
Figure 8. Stereomicroscope images of PLGA foams with microspheres	51
Figure 9. SEM images of PLGA foams with microspheres.	52
Figure 10. Pore size distribution of foams	53
Figure 11. Cell proliferation curves in BMP (+) and BMP (-) foams.	55
Figure 12. ALP activity in BMP (+) and BMP (-) foams.	57
Figure 13. Percent ALP activity increase in BMP (+) and BMP (-) foams. ..	59
Figure 14. ALP activity difference between BMP (+) and BMP (-) foams. ..	60
Figure 15. Specific ALP activity in BMP (+) and BMP (-) foams.	61
Figure 16. Specific ALP activity difference between BMP (+) and BMP (-) foams.	63
Figure 17. Phalloidin staining of cells observed with confocal laser scanning microscopy	64
Figure 18. SEM images of cell seeded and unseeded F-7 (-) after 21 days of culture	66
Figure 19. SEM images of cell seeded F-2&7 (+) after 21 days of culture.	67

Figure A-1. BSA calibration curve prepared with microBradford assay for encapsulation efficiency study.	90
Figure B-1. BSA calibration curve prepared with microBradford assay for release study.	91
Figure C-1. Calibration curve for BMSCs prepared by Alamar Blue Assay..	92
Figure D-1. ALP calibration curve prepared with p-nitrophenol.....	93

LIST OF ABBREVIATIONS

ALP	Alkaline Phosphatase
BMSCs	Bone Marrow Stem Cells
BMPs	Bone Morphogenetic Proteins
BSA	Bovine Serum Albumin
CLSM	Confocal Laser Scanning Microscope
DMEM	Dulbecco's Modified Eagle's Medium
ECM	Extracellular Matrix
ECSs	Embryonic Stem Cells
F	Foam
F-2 (+)	BMP-2 loaded microsphere containing foam
F-2 (-)	BMP-2 unloaded microsphere containing foam
F-7 (+)	BMP-7 loaded microsphere containing foam
F-7 (-)	BMP-7 unloaded microsphere containing foam
F-2&7 (+)	BMP-2 and BMP-7 loaded microspheres containing foam
F-2&7 (-)	BMP-2 and BMP-7 unloaded microspheres containing foam
F-4	Foam loaded with 4% microspheres
F-10	Foam loaded with 10% microspheres
F-4&10	Foam loaded with 4% and 10% microspheres
FCS	Fetal Calf Serum
FGF-2	Fibroblast Growth Factor-2
FSCs	Fetal Stem Cells
FITC	Fluorescein Isothiocyanate
HAP	Hydroxyapatite
IGF	Insulin-like Growth Factor
MS	Microspheres
MSCs	Mesenchymal Stem Cells
P ₄ VN	Poly(4-vinyl pyridine)
PB	Phosphate Buffer
PCL	Poly(ϵ -caprolactone)
PEG	Polyethylene glycol

PGA	Poly(glycolic acid)
PHAs	Polyhydroxyalkanoates
PHB	Poly(3-hydroxybutyrate)
PHBV	Poly(3-hydroxybutyrate-co-3-hydroxyvalerate)
PLA	Poly(lactic acid)
PLGA (50:50)	Poly(lactic acid-co-glycolic acid) (50:50)
PPF	Poly(propylene fumarate)
RGD	Arginine-Glycine-Aspartic acid
rhBMP-2	Recombinant Human Bone Morphogenetic Protein-2
rhBMP-7	Recombinant Human Bone Morphogenetic Protein-7
SEM	Scanning Electron Microscope
TCPS	Tissue Culture Polystyrene
TGF- β	Transforming Growth Factor-beta
Trypsin-EDTA	Trypsin-ethylenediamine tetraacetic acid
VEGF	Vascular Endothelial Growth Factor

CHAPTER 1

INTRODUCTION

1.1 Tissue Engineering

Tissue engineering is an emerging interdisciplinary field which combines the principles of biology, chemistry and engineering to support, restore, repair or regenerate a portion of or a whole tissue [1].

Tissue engineering is currently one of the most intensively studied fields since it offers a great promise in the treatment of various severe defects of different tissue types where regular applications like surgery or drug administration is ineffective or inappropriate. Notably, cases which essentially require organ transplantation have high expectations of tissue engineering since donor insufficiency is a major problem.

Cells constituting a tissue reside in a complex structure called extracellular matrix (ECM) which is deposited by the cells during tissue formation. The ECM plays a vital role in maintenance of the structure and function of the tissue. One of the major goals of tissue engineers is to create structures that can closely mimic the ECM.

Porous, biocompatible and preferentially biodegradable or bioresorbable scaffolds that would mimic the extracellular matrix and thus act as a supportive bed for the immigration and ingrowth of nearby cells but carries no cells of its own is an acellular approach of tissue engineering [2]. Biocompatibility is an essential feature of the materials used in tissue engineering as it is in all biomedical applications. A biocompatible material does not introduce toxic effects to the body and is compatible with the surrounding tissue and body fluids and maintains its properties in the biological medium. for a predetermined service life.

Biodegradation is another key feature that a scaffold material preferentially possesses. The term 'biodegradable' defines materials which are subject to degradation in the biological system. A scaffold which degrades in a period paralleling cell proliferation and natural ECM deposition achieves complete replacement of the implant with the natural tissue [3].

Another acellular approach involves the use of cell carriers containing certain bioactive agents to enhance or induce immigration, proliferation and/or differentiation of nearby cells at the implant site. These bioactive agents can directly be incorporated to or immobilized on the scaffolds by covalent or non-covalent bonding, before transplantation [2].

However, the most promising application of tissue engineering involves cellular systems. Although the term 'tissue engineering' involves all of the above mentioned approaches; the design of 3D living cellular constructs which combine the use of scaffolds, cells and certain bioactive agents together is the most promising approach in bone tissue engineering as well as in other tissue types. The types of cells used in these kind of applications could differ from each other in terms of type and source.

1.1.1 Bone Tissue Engineering

Bone defects occur due to a variety of reasons including trauma, congenital deformity or pathological deformation [4]. The currently used surgical approaches for the treatment of bone defects include use of biomaterials as bone substitutes and grafting procedures which allow replacement of the defective sites with functional and viable alternatives harvested from healthy sites of bone tissue of animals [1, 5]. Biomaterials that are used as bone substitutes can be metals, polymers, ceramics and composite materials [6]. However the use of non-living bone substitutes has several potential risks of failure. Corrosion, wear or fracture of these materials could result in their incompatibility and consequent failure. Secondly, their inability to integrate with the surrounding medium may result in an immunogenic response leading to inflammation at the implant site [7].

Another concern is that although these artificial substitutes can display osteoconductive properties (enable bone ingrowth) they do not display osteoinductive properties (stimulate bone formation) which results in limitation of repairing process and full restoration of function at the defect site [2, 8]. Finally, these materials lack the ability of remodeling, thus they cannot adapt to the aging of the patient.

The grafts can be classified into three groups depending on the donor type. When the donor is the patient himself, it is defined as an autograft. When the donor is another human being, it is an allograft. If however, the donor is a member of another species, then it is a xenograft. Each of these procedures have their own constraints [9].

Autografts are promising because of their immunocompatibility; however, they have several disadvantages and health risks of which some can be very critical. One of the major risks of autografts is the morbidity caused at the donor site. In addition, the quantity of donor tissue is limited. Finally, the inconvenience and the risk of the second surgery is another disadvantage of these grafts [1].

The allografts or xenografts on the other hand have disadvantages and health risks such as rejection immunogenic response leading to an inflammation at the site of implantation [4]. Although certain chemical and physical treatments reduce there still is the risk of transmittence of donor pathogens [4].

All of the limitations associated with grafts and bone substitutes have led the scientists to search for alternative treatments for severe bone defects. Tissue engineering with 3D cellular constructs carrying certain bioactive agents can benefit from the advantages and avoid the disadvantages associated with artificial bone substitutes and grafts.

1.2 Scaffolds in Bone Tissue Engineering

Scaffolds are one of the two major components of a tissue engineering construct. There are certain features that a scaffold should possess in order to assure that it meets essential requirements for bone regeneration. Biocompatibility is the most crucial requirement. Degradability in the biological environment is another essential feature and should be in accordance with the growth of natural bone tissue. The degradation rate of the scaffold material can be altered through changes in the chemistry, addition of other components such as ceramics [10, 11] or by altering the manufacturing methods [11-13] to obtain more appropriate degradation profiles.

Porosity is another critical requirement. When engineering a tissue, porous scaffold structures displaying an interconnected porosity are necessary for cell migration, proliferation, vascularization as well as transport of nutrients and waste materials. Former studies have reported that the macroporosity should be in the range of hundred microns considering the size of osteoblasts and blood vessels; on the other hand, microporosity (pores below 10 μm) is also important since it favors protein adhesion, cell attachment and proliferation [14-16]. Many studies have shown that pore size, shape and density of scaffolds have a significant effect on the behavior of cells [16, 17]. Porosity also improves the ability of the scaffold material to interlock with the surrounding natural bone tissue enhancing the mechanical stability at the interface [16].

Mechanical strength of a scaffold could be crucial in bearing the load endured by the bone depending on the site of use [18].

Surface chemistry and topography of scaffolds are very important in cell-material interactions. Certain treatments such as exposure to UV, plasma, grafting of chemical and biological entities are applied to modify the surface properties of scaffolds.

For example, Arg-Gly-Asp (RGD) sequence carrying peptides which are involved in integrin-mediated cell adhesion are incorporated into the structure of the scaffolds [19]. In other applications short peptide sequences carrying the RGD are grafted on the existing scaffold [20].

Scaffolds in bone tissue engineering can be manufactured in the form of films, foams and fibers through the use of methods like freeze drying, fiber bonding, solvent casting, particulate leaching, membrane lamination, electrospinning, photolithography and melt molding [21, 22].

1.2.1 Natural Polymers as Scaffold Materials

The two main advantages of using natural polymers (collagen, fibrin, chitosan, alginate, etc...) as scaffold materials are their biodegradability and biocompatibility. However, their low mechanical strength could be a disadvantage in load bearing applications. In order to overcome this, their structures are strengthened by crosslinking with appropriate chemicals [4] or composite formation with the addition of ceramics such as hydroxyapatite [23].

Collagen, fibrin, chitosan, alginate, silk, hyaluronic acid and microbial polyesters (polyhydroxyalkanoates) are among the most commonly used polymers of natural origin which can be used as is or in composite form after blending [24].

Collagen is the naturally secreted main organic component of basic bone cells namely osteoblasts. It is also known to be the most abundant ECM component in body and is therefore widely studied as a scaffold material in bone tissue engineering [4, 25, 26]. Collagen can be isolated and purified from xenogeneic sources such as porcine skin and cow hide and shaped into membrane films, sponges, threads and acidic hydrogels [9]. The low mechanical properties of collagen are generally overcome by crosslinking [4].

Fibrin is a polypeptide which has an important role in wound healing. It is formed by the self assembly of fibrinogen molecules during clotting upon a blood vessel injury.

Fibrin can either be obtained directly from blood clots or by processing of commercially available fibrinogen isolated from blood plasma. In the case of patient-specific treatments, even the patient's own blood can be used as the fibrinogen source; eliminating the risks of disease transmission and immunogenic reactions [27].

Chitosan is a deacetylated chitin derivative that is mostly found in shells of marine crustaceans and fungal cell walls. This linear polysaccharide which is a copolymer of glucosamine and N-acetyl-D-glucosamine linked in a β (1-4) manner is extensively studied due to its positive charge, biodegradability, high biocompatibility and ease of processing. Moreover, physicochemical and biological properties of chitosan can be altered by varying the degree of deacetylation [28]. This enables tailoring of the polymer for the different goals in bone tissue engineering.

Alginate, as a linear polysaccharide composed of β -D-mannuronic acid and a (1-4) linked α -L-gluronic acid is another natural polymer used in bone engineering. Alginate can be crosslinked in the presence of multivalent cations such as Ca^{+2} , to create scaffolds [29].

Silk is a fibrous protein produced in fiber form by silkworms and spiders. It is being used clinically as a suture material for centuries. The considerably high mechanical strength of silk has made it a potential biomaterial to be used as a scaffold in bone tissue engineering. It has been processed into sponges, films, hydrogels and electrospun non-woven mats. It is also possible to modify surface characteristics of silk by chemical immobilization or physical adsorption of certain peptides such as RGD [30, 31].

Hyaluronic acid is a linear, high molecular weight biopolymer found in all connective tissues in the body. It is known to be a major component of ECM with viscoelastic properties and ability to bind specifically to proteins in the ECM and on the cell surface. It also plays a role in certain biological processes like morphogenesis, wound repair and inflammation and all these have made it a promising scaffold material [9, 32, 33].

Polyhydroxyalkanoates (PHAs) are polyesters which are produced by microorganisms under unbalanced growth conditions [34]. PHAs which have been reported to be suitable for tissue engineering involve; poly (3-hydroxybutyrate) (PHB), copolymers of 3-hydroxybutyrate and 3-hydroxyvalerate (PHBV), poly(4-hydroxybutyrate) (P4HB), copolymers of 3-hydroxybutyrate and 3-hydroxyhexanoate (PHBHHx) and poly (3-hydroxyoctanoate) (PHO) [34]. They generally are known to be thermoprocessable and biodegradable via hydrolysis . Among the PHAs; PHB is of particular interest owing to its previously reported consistent bone tissue adaptation response [35] and ability to support *in vitro* bone formation [36, 37]. Various PHAs can be blended among themselves to yield dramatically different material properties. The disadvantages associated with some of these PHAs is their limited availability, time-consuming procedure of extraction from bacterial cultures and remaining pyrogens [34].

1.2.2 Synthetic Polymers as Scaffold Materials

The advantages of synthetic polymers over natural polymers can be stated as a lower risk of immunogenicity and disease transmission, easier processibility, higher flexibility for tailoring to obtain a variety of mechanical and chemical properties which would improve mechanical strength, degradation rate and interaction with the cells. This can be achieved by altering the chemical composition, molecular weight, and addition or removal of functional groups [4].

Among the most common synthetic polymeric materials are, poly(ϵ -caprolactone) (PCL), poly(glycolic acid) (PGA), poly(lactic acid) (PLA), their copolymers poly(lactic acid-co-glycolic acid) (PLGA) as bulk degradable polymers, poly(phosphoesters), poly(phosphazene), and poly(propylene fumarate) (PPF) [38].

PLA, PLG and their copolymer PLGA are FDA approved and partly because of that they are the most intensively investigated synthetic polymers in bone engineering. These polymers undergo bulk degradation via hydrolysis of ester bonds upon water uptake.

The degradation products of this process are lactic and glycolic acid, acidic small molecules that can be removed from the body via natural metabolic routes [38]. However, since these degradation products are acidic in nature, the lowered pH around the scaffold poses a risk for the cells. In order to solve this problem certain basic compounds such as bioactive glasses and calcium phosphates can be incorporated into the structure to stabilize the pH around the scaffold [39-41]. Many studies have been conducted using this kind of composite scaffolds which will be discussed further in the following section.

PLA exists in three forms: L-PLA (PLLA), D-PLA (PDLA) and racemic mixture of D,L-PLA (PDLLA). Each of these differs from the others in stereochemistry and as a result in degradation kinetics. PGA is more hydrophilic and degrades faster when compared to PLA. PLLA is highly crystalline and degrades much more slowly when compared to amorphous PDLLA due to reduced water permeation [38].

PLGA is the most intensively studied member of the polyester family for bone tissue engineering [42-45]. Its degradation rate varies depending on the ratio of lactic acid and glycolic acid in its structure. Therefore it is possible to choose the correct PLGA for a given application by just looking at its composition. For instance, blends containing a higher amount of PGA are known to have a faster degradation profile [39].

Polycaprolactone (PCL) is also a linear polyester but possesses a much slower rate of degradation which can be several years in vivo which makes it a suitable candidate for bone tissue engineering especially for critical sized large and difficult defects where slower degradation is preferred [46, 47].

Polypropylenefumarate (PPF), is an unsaturated polyester which can be crosslinked in situ owing to the presence of the double bond along the backbone of repeating units and hardens upon crosslinking. This property of PPF makes it a suitable injectable bone fixation [48]. PPF undergoes hydrolysis with the release of propylene glycol and fumaric acid both of which can be removed from the body through natural pathways [38].

Poly(phosphoester) and poly(phosphazene) are highly hydrophobic, and therefore, are surface eroding synthetic polymers. This property has made them promising scaffold candidates in the field of tissue engineering since the mass to volume ratio is maintained during the degradation process which prevents any catastrophic failures as encountered with bulk degrading polymers such as PLGA. The potential risk of acidic degradation products is minimized owing to their lower concentration [38].

1.2.3 Ceramics and Composites as Scaffold Materials

Ceramics are also known to be used as scaffold materials in bone tissue engineering. These ceramics can either be calcium phosphates or bioactive glasses. Calcium phosphate ceramics mainly involve hydroxyapatite (HAP), beta-tricalcium phosphate (β -TCP), biphasic calcium phosphate (BCP), amorphous calcium phosphate (ACP), carbonated apatite (CA) and calcium deficient HAP (CDHA) [23]. Bioactive glasses are a group of glass compositions which were discovered in 1969 to be perfectly biocompatible and display ability to bind to the bone [49, 50]. Most of the bioactive glasses are constituted of SiO_2 , Na_2O , CaO and P_2O_5 [38].

Ceramics can be designed as scaffolds with interconnected porosity by using techniques such as leaching and sintering out of salt crystals or polymeric microparticles [23].

Natural bone has organic compounds and inorganic compounds. Since the main inorganic compound of bone is partially carbonated HAP, HAP and other calcium phosphates are being extensively studied in bone tissue engineering. They are osteoconductive and have the ability to bind to bone. There have been various studies which confirmed that independent of their form and phase, calcium phosphates support attachment of osteoblasts and stem cells [51].

Bioactive glasses are reported to be bioactive due to their ability to bind to bone. This process happens due to formation of a CaP-rich layer which then crystallizes to carbonated hydroxyapatite on the surface of the glass after implantation and contact with biological fluids [23]. Several studies have shown that bioactive glasses support *in vitro* osteoblast attachment, proliferation and differentiation of mesenchymal cells into osteoblasts. [52-54].

Although ceramics seem to be excellent materials for use as scaffolds, they possess certain drawbacks. Brittleness and slow or no degradation and resorption are the main issues. In order to overcome these drawbacks ceramics are generally manufactured as composites, mostly of polymer-ceramic type. Addition of biodegradable polymers in the structure aims to improve the degradability, alter the mechanical properties of ceramics and create a porous structure. These composites also mimic the natural bone tissue composition of collagen and calcium phosphate. Several studies have reported the success of such designs in bone tissue engineering with better mechanical, osteoconductive and osteoinductive properties [23].

1.3 Stem Cell Based Bone Tissue Engineering

Stem cells are unspecialized cells which have the ability of self renewal and differentiation into multiple cell lineages. Stem cells can be isolated from three main sources: embryonic, fetal or adult tissues.

Embryonic stem cells (ESCs) are derived from the inner mass of the blastocyst, preimplantation in the uterine wall. They are referred to as pluripotent due to their potential to form any adult cell type derived from the three embryonic germ layers; mesoderm, endoderm and ectoderm. These cells can be isolated from early human embryos and cultured for long periods and manipulated towards differentiation into a wide array of cell types [55]. Fetal stem cells (FSCs) derived from the developing organs from a fetus also have an excellent proliferative potential and the ability to differentiate into many cell types. Although ESCs and FSCs seem to possess a great potential in tissue engineering, there are many unresolved ethical issues regarding their use. Therefore, stem cell based tissue engineering is currently focused on adult stem cells derived from adult tissues.

Adult stem cells are generally referred to as mesenchymal stem cells (MSCs). MSCs are found in different tissue types including adipose tissue, muscle, bone marrow and trabecular bone. These cells are said to be multipotent; they have the potential to differentiate into multiple organ specific cell types [56]. They are responsible of replacing the worn out cells in the tissue they reside in by differentiating into those specific cell types. Their potential to differentiate into cell lineages belonging to tissues other than their tissue of origin is still being investigated. This ability is referred to as 'plasticity'. It is a controversial issue under investigation [57].

MSCs can be isolated and cultured under laboratory conditions. They can rapidly proliferate and be guided by extracellular signals such as growth factors, towards differentiation into multiple cell types. Bone marrow is the main and the most frequently utilized source of MSCs for preclinical and clinical studies.

Bone marrow is the reservoir for two main types of stem cells. The first population is hematopoietic stem cells which are responsible from reconstitution of the hematopoietic system by giving rise to cells of all blood lineages. The other population is referred to as non-hematopoietic stem cells which possess great proliferative potential and the ability to differentiate into different cell types including osteoblasts, adipocytes, myoblasts and chondrocytes [58, 59]. This section is concentrated on the latter population which has osteogenic potential, and therefore, is relevant with stem cell based bone engineering.

German pathologist Julius Cohnheim was the first scientist to suggest that non-hematopoietic stem cells were present in bone marrow. His suggestion was then verified by Alexander Friedenstein who isolated these cells displaying fibroblast-like morphology from bone marrow, characterized them and discovered that these cells could be grown *in vitro* and be manipulated to differentiate into osteogenic progeny.

Later, Owen and colleagues demonstrated that intraperitoneal implantation of bone marrow derived stem cells enclosed in a porous membrane could generate bone and cartilage in host animals [60].

Non-hematopoietic bone marrow stem cells (BMSCs) can be isolated from the superior iliac crest of the pelvis or tibial and femoral marrow compartments through a bone marrow aspirate [61-63]. They can be distinguished from non-adherent hematopoietic cells by their fibroblast-like morphology and high adherence to tissue culture plates [64, 65]. These stem cells constitute only a very small fraction of the total population of nucleated cells in bone marrow. Following their isolation they should be expanded *in vitro* to obtain larger numbers [62]. Moreover; studies have reported that *in vitro* expanded BMSCs favor more rapid uniform bone formation [66, 67].

The osteogenic differentiation of BMSCs can be subdivided into three stages, proliferation, ECM synthesis, maturation and mineralization. [56]. This process requires certain biological signals to trigger a cascade of intracellular pathways and lead to osteogenic differentiation. Among the several bioactive signalling agents there are bone morphogenetic proteins (BMPs) which are members of the transforming growth factor (TGF) superfamily and also fibroblast growth factors which play a major role in this osteogenic differentiation process.

In order to prove osteogenic differentiation several markers are taken into consideration including alkaline phosphatase, collagen I, osteocalcin, bone sialoprotein, osteonectin and osteopontin [59].

The fact that high differentiation potential possessing BMSCs can easily be isolated and expanded *in vitro* has made them very attractive tools for bone tissue engineering applications [68]. Moreover, studies suggest that these stem cells have highly reduced immunoreactivity or they even may be totally non-immunogenic [69-72]. This property makes the clinical use of allogenic BMSCs possible for treatment of severe bone defects. Another important feature of BMSCs is their resistance to low oxygen conditions.

Following implantation of a porous scaffold at the site of defect, rapid vascularization of the scaffold material is necessary to ensure viability of preseeded and immigrating cells. However, this process might not be as rapid as desired. At this point the low oxygen resistance of BMSCs can be a major advantage in tolerating the slower vascularization rate [73].

BMSCs can be used clinically by systemic intravenous or local percutaneous bone marrow aspirate injections for treatment of certain bone defects such as delayed or non-union fractures or genetic bone diseases. Examples include, successful stimulation of healing in non-union fractures following local percutaneous bone marrow aspirate injection [74] and improved clinical conditions in patients with severe Osteogenesis Imperfecta following intravenous injection with allogeneic BMSCs [75].

However, such treatments can sometimes fail and be unsuccessful in the production of relevant and durable clinical effects [68].

Large bone defects also require treatment other than intravenous or subcutaneous BMSC injection. These are the stem cell based bone tissue engineering approaches which involve stem cell seeded biomaterial scaffolds.

As mentioned before, BMSCs constitute only a very small fraction of the total population of nucleated cells in the bone marrow; therefore, they must be cultured *in vitro* until a sufficient quantity is obtained prior to their clinical use. However, it is known that, during this culturing period BMSCs can lose their differentiation potential [68]. This can be a major problem especially with elder patients who possess even a lower number of BMSCs. Although this finding appears discouraging, it has been reported that the use of biomaterial scaffolds in BMSC culturing results in the retention of osteogenic differentiation potential [76]. There are many reports about the success of BMSC loaded porous scaffolds in healing large bone defects [77-79] and this supports the idea that bone tissue engineering via scaffolds is the most promising therapeutic approach for treating bone defects.

1.4 Bioactive Agents in Bone Tissue Engineering

Bone formation is a complex process which includes a cascade of events mediated by hormones, cytokines and growth factors. These are the signaling molecules which regulate cell adhesion, migration, proliferation and differentiation. For instance, it is known that locally produced cytokines and growth factors promote migration of osteoprogenitor cells to the site of defect following a bone fracture and direct their proliferation, ECM synthesis and osteogenic differentiation [80]. They could promote and/or prevent the above mentioned events by up- or down-regulating synthesis of certain proteins, growth factors and receptors [7].

The effect of these molecules is mediated by the surface receptors of the target cells. Following their recognition and binding by surface receptors, they activate intracellular phosphorylating enzymes which then trigger certain signaling pathways by aggregation of different proteins and co-factors. These proteins and co-factors migrate to the nucleus and with participation of other transcription factors, they up- or down-regulate the expression of certain genes which results in specific cellular activity or phenotype changes [81].

Large amounts of recombinant growth factors can be manufactured owing to the advances in cloning technology. These commercial products possess pharmaceutical qualities which enable their local delivery in tissue engineering applications. Since each of these molecules possesses distinct efficacies and potencies, different levels of bone healings are reported. Moreover, the variations in defect size, bone type, physiological systems of modeling species make optimization of local delivery strategies very challenging [4].

The most commonly used bioactive agents in bone tissue engineering include insulin-like growth factor (IGF), fibroblast growth factor-2 (FGF-2), vascular endothelial growth factor (VEGF), transforming growth factor- β (TGF- β), and bone morphogenetic proteins (BMPs).

It is known that IGF plays an important role in bone metabolism [82]. It is an endocrine, paracrine and autocrine inductive molecule which mediates growth factor, cytokine, hormone and morphogen activities during bone fracture healing [83]. IGF is a single chain peptide and exist as two isoforms which are IGF-I with 70 amino acids and IGF-II with 67 amino acids [81]. Systemic application of IGF-I rapidly activates bone turnover which can be detected by increased serum levels of bone formation markers such as osteocalcin [81]. Owing to its significant role in bone repair, IGF is one of the most commonly utilized growth factors in bone tissue engineering studies.

FGF-2 is a component of the bone matrix and its stimulatory effect on bone healing is being intensively studied. It has been reported that exogenous addition of FGF-2 to a bone defect site accelerates bone repair and remodeling [84] but this positive effect is being contested. Several studies have demonstrated that FGF-2 has an inhibitory effect on osteogenic differentiation of bone marrow stem cells [85, 86], while other studies have reported that the positive effects observed are dose and duration dependent [87, 88].

VEGF is the main growth factor which mediates vasculature via stimulating proliferation and migration of endothelial cells [89]. Bone is a highly vascularized tissue and rapid vascular ingrowth is necessary during bone healing. Also, the viability of transplanted cells and cells migrating to the scaffold from the nearby sites of host tissue are dependent on vascularity of the region. Cells deprived of blood flow and thus oxygen, are destined to die. Studies have suggested that blood vessels would infiltrate a porous scaffold eventually but the complete penetration of vascular tissue might take 1-2 weeks a far too long period for an ischemic implant to stay viable [90, 91]. In order to accelerate vascularization it is highly common to incorporate VEGF into scaffolds [89]. Stimulation of proliferation and migration of endothelial cells by VEGF results in the formation of tubular blood vessels. This is the primary action of VEGF, however, there are also studies demonstrating that VEGF has a positive effect on recruitment, survival, and activity of bone forming cells [92]. It is therefore a very commonly used molecule in bone tissue engineering studies.

TGF- β family includes more than thirty structurally similar proteins. These molecules display multiple functions including stimulation of cell recruitment, proliferation, ECM synthesis and osteogenic differentiation [93-95]. TGF- β family is divided into two main groups. The first group includes TGF- β s themselves and other proteins such as activins while the second one comprises BMPs (see following section) [96]. TGF- β itself is being studied intensively as an osteoinductive molecule for bone engineering applications owing to its proliferative and osteoinductive effects on MSCs [97-99].

1.4.1 BMPs in Bone Tissue Engineering

Most of the research on effect of bioactive agents in bone engineering is focused on BMPs. They are regulatory molecules involved in skeletal tissue formation during embryogenesis, growth, adulthood, and healing [100].

The presence of a novel osteoinductive molecule in the matrix which stimulates osteogenic differentiation of precursor cells was first suggested by Urist in the mid-60s following his study which demonstrated induction of new bone formation from a decalcified bone matrix [101]. Several years later this factor was named as Bone Morphogenetic Protein (BMP) by Urist and Strates [102]. Since then more than 40 types of BMPs have been identified. BMPs are dimeric molecules with two identical polypeptide chains of more than 400 amino acids linked by a single cysteine binding disulfide bond [103]. Their primary structure shows 40–50 % similarity with TGF- β [104]. They can be isolated from bones of various mammals including bovine, mouse, rat, horse and human. Moreover, recombinant human BMPs are becoming commercially available products which are devoid of impurities and thus do not carry the risk of xenogenic reaction.

BMPs act by activating specific transmembraneous heterogenic receptor complexes located on the cell surface. Following binding, these activated receptors phosphorylate specific intracellular messenger proteins called Smads.

Following their translocation to the nucleus, Smads bind to specific DNA sequences, interact with other DNA-binding proteins and attract transcriptional co-activator/receptors and thus regulate transcription of the target genes involved in various cellular responses which include chemotaxis, proliferation, ECM production, osteogenic differentiation and vascular invasion [104].

Various preclinical studies with rats, rabbits, dogs, sheep and non-human primates investigating the osteoinductive effects of BMPs have demonstrated bone formation at large critical sized and bone defects implanted with BMP carrying matrices [105-108].

1.4.1.1 BMPs in Osteogenic Differentiation of MSCs

BMPs are known to be important regulators of proliferation and osteogenic differentiation of MSCs [109]. BMP induced osteogenic differentiation occurs as a sequence of cellular events beginning with chemotaxis and proliferation of MSCs. MSCs then differentiate into chondroblasts which undergo hypertrophy and calcify the matrix leading to osteogenic differentiation and replacement of cartilage with bone [103]. The concentration and continuous presence of BMPs in the environment is very important during this event. It has been demonstrated that withdrawal of BMPs during this cascade can result in the loss of the osteogenic differentiation potential [110]. BMP regulated direct osteogenic differentiation of MSCs by-passing the chondrogenic differentiation step, has also been demonstrated by a variety of *in vitro* studies with elevated concentrations of BMPs [104].

Recombinant Human Bone Morphogenetic Protein-2 (rhBMP-2) and Recombinant Human Bone Morphogenetic Protein-7 (rhBMP-7) are the only FDA approved members among the BMP family that have currently been developed for clinical use. Their success in MSCs proliferation and osteogenic differentiation *in vitro* and bone defect healing *in vivo* is well established [103, 104, 111].

1.5 Delivery of Bioactive Agents in Bone Tissue Engineering

Systemic or local percutaneous injection of bioactive agents at the site of defect is an undesired approach due to short biological half-life of growth factors (their susceptibility to enzymatic degradation), lack of long term stability, tissue specificity, potential dose dependent carcinogenicity and rapid diffusion away from the site of application. Each of these conditions would decrease the effect of bioactive agents leading to failure in bone generation [112].

Controlled delivery is the term used to define systems that are capable of delivering certain molecules at a determined release rate achieving prolonged availability of bioactive agents [113]. The drawbacks associated with systemic or percutaneous injection based administration have necessitated development and utilization of local and controlled release achieving systems for safe, efficient and prolonged availability of bioactive agents in many illnesses.

Controlled delivery is applicable to tissue engineering mainly for the delivery of growth factors. There are different strategies utilized for incorporation of these agents in the scaffolds to achieve retention of bioactive agents at the implantation site for efficient and prolonged effects.

1.5.1 Delivery of Multiple Bioactive Agents

Bone formation and repair is a complex cascade of events during which multiple growth factors are involved. Therefore; one of the key goals in bone tissue engineering approaches may be the controlled delivery of combinations of growth factors from appropriate scaffold designs. The significance of enhanced osteogenic effect with multiple growth factors has been well established by a comprehensive study which investigated role of different BMPs in osteogenic differentiation [114]. The study was conducted with stem cells which displayed adenovirus-mediated BMP expression.

The results demonstrated that certain BMPs with very low or none osteogenic activity exhibited strong osteogenic activity when they were co-expressed in stem cells [114]. Various studies have supported these findings by enhanced bone formation upon administration of dual growth factors. For instance, it was demonstrated that dual delivery of TGF- β 3 and BMP-2 from alginate scaffolds significantly enhanced *in vivo* bone formation when compared to single growth factor loaded scaffolds [115].

It is very crucial that proper combinations of growth factors are selected for multiple delivery strategies. Studies have demonstrated that application of multiple growth factors can exert both positive and negative effects depending on the choice of combinations. For instance a study has reported decreased bone formation with a BMP-2 and bFGF incorporated collagen sponge implanted in a tibia fracture site [116] whereas another one has reported enhanced bone formation with combined application of TGF- β 1 and IGF-1 when compared to their single applications [117].

Not only combined but also sequential delivery of certain bioactive agents may also be a promising approach since bone formation and repair is a cascade of events with appearance and disappearance of multiple bioactive agents at different stages with different concentrations. A dual and sequential delivery approach may also eliminate the risk of previously mentioned negative interference of multiple growth factors with each other. Moreover, such an approach would elicit prolonged availability of bioactive agents during the osteogenic differentiation process. This can be crucial since it has been suggested that stem cells can lose their differentiation potential if certain growth factors are not available in the medium [110]. The positive effects of sequential delivery of two growth factors mainly BMP-2 and IGF-1 has been well demonstrated with accelerated and enhanced osteogenic differentiation of BMSCs when compared to simultaneous delivery performing control groups [118].

It has been suggested that multiple delivery of growth factors might yield positive results with reduced amounts of growth factor utilization when compared to positive results obtained with much higher loading doses administered in single growth factor delivery approaches [115]. This is probably due to increased osteogenic potency of growth factors when they are employed in combinations. This can be a major advantage when the high costs of growth factors are considered.

1.5.2 Incorporation of Bioactive Agents into Scaffolds

Bioactive agents can be incorporated into scaffolds either directly by themselves or in micro- and nanoparticles.

1.5.2.1 Direct Incorporation of Bioactive Agents into Scaffolds

Bioactive agents can be directly introduced to scaffolds by covalent or non-covalent bonding. Non-covalent binding approaches include physical entrapment, surface adsorption through physico-chemical interactions, affinity binding or ionic complexation. Entrapment of bioactive agents in polymeric scaffolds yields a diffusion mediated release with or without accompanying biodegradation of the scaffold. Release in surface adsorption-based immobilization approaches is achieved through environment sensitive desorption [112]. Although adsorption is a very simple method, limited control in release behavior and conformational changes leading to denaturation of the bioactive agent can be two major disadvantages encountered in this approach. Ionic complexation based entrapment is possible for proteins with different isoelectric points which can bind to charged natural polymers like alginate and chitosan or synthetic polyelectrolytes. Release from such systems is dependent on the environment sensitivity such as salinity, pH, etc. Covalent binding of bioactive agents to scaffolds can be achieved via linkers or by direct coupling. However, the preservation of biological activity of these bioactive agents is an important issue that must be considered when designing such systems [112].

Chemical modifications of bioactive agents by succinylation, acetylation, biotinylation and truncation can also be performed to enhance their affinity, stability and bioactivity [112].

The release rates and amounts of bioactive agents from scaffolds can be controlled by varying the immobilization method, loading and/or three dimensional structure of the scaffold, mainly geometry, volume, porosity, biodegradation rate and hydrophobicity.

Pore size dependent control of rhBMP-2 release from PLGA scaffolds [119] and biodegradation dependent release of TGF- β from collagen sponges by altering the extent of crosslinking [120] are two examples of controlled release kinetics of bioactive agents directly incorporated in scaffolds.

1.5.2.2 Micro/Nanoparticle Mediated Delivery from Scaffolds

Entrapment of bioactive agents in micro- and nanoparticles incorporated into scaffolds is a novel approach. Such an approach enables improved control on release kinetics and protection from non-specific or specific degradation of bioactive agents upon implantation. Micro- and nanoparticles can be prepared from degradable or non degradable, natural or synthetic polymers, as homopolymers, copolymers, physical polymer blends and polyelectrolyte complexes [121].

The two main micro- and nanoparticle manufacturing methods include internal gelation [121,122] and solvent evaporation either by a double emulsion or single emulsion approach [123]. Internal gelation is a process which defines crosslinking dependent gelation of polymers. Solvent evaporation is based on organic solvent evaporation from dispersed oil droplets of polymer and bioactive agent [124].

Release from particles can be diffusion, swelling and/or biodegradation mediated. Diffusion mediated release occurs due to the movement of bioactive agents through the pores of the particle. The rate is dependent on porosity, diffusion coefficient of the agent in the aqueous medium, partition coefficient of the bioactive agent, dose and distribution of bioactive agent within the particle thus the diffusional distance [112,124]. Biodegradation mediated release occurs when biodegradable polymers are utilized in particle preparation. In such cases, release of the physically immobilized bioactive agent from the particle occurs due to the hydrolytic or enzymatic breakdown and dissolution of the polymer. Release kinetics from biodegradable systems can be controlled by altering the degradation profile of the polymers.

Swelling based release occurs in hydrogel particles. Hydrogels are crosslinked hydrophilic networks which absorb large amounts of water and swell [4]. This swelling behavior leads to diffusion-mediated release of bioactive agents through the enlarged pores of the particle. The release rate in such systems can be controlled by altering the extent of crosslinking and thus the degree of swelling [125].

The general release profile of particles consists of an initial burst with the release of a high percentage of the total drug content followed by a slower and more constant release rate. The burst effect is due to the rapid release of the bioactive agents located at the particle surface, the following slower release rate is mediated by either of the above mentioned mechanisms [124]. Different approaches can be utilized to minimize the burst effect and obtain more constant release profiles as in the case of increasing drug concentration from the periphery towards the center of the particle [126] or by forming of an outer skin with low porosity [127].

Particles carrying bioactive agents can be directly introduced to porous scaffolds by absorption [128,129] or direct mixing with the polymer solution prior to scaffold production [130,131].

The major goal in particle mediated release is to prolong bioactive agent availability, have improved control on release kinetics and enable protection of the bioactive agent from physiological fluids and biodegradation products of the scaffold. Owing to these advantages addition of bioactive agents to the 3D design via particles is more promising in terms of efficient bioactive delivery when compared to their direct incorporation into scaffolds. A recent study has demonstrated significant *in vivo* bone formation following implantation of nanofibrous scaffolds incorporating BMP-7 nanospheres, whereas BMP-7 adsorbed scaffolds failed to induce bone formation due to possible loss of biological activity or insufficient duration at the implant site (129). Another example is enhanced bone formation with BMP-2 nanoparticles incorporated in a fibrin gel when compared to BMP-2 loaded fibrin gels [132].

1.6 Scope of the Study

The aim of this study was to develop an implantable, sequential delivery executing system for bone tissue engineering. The system was constituted of bioactive agent loaded complexed microspheres embedded in cell seeded porous polymeric scaffolds.

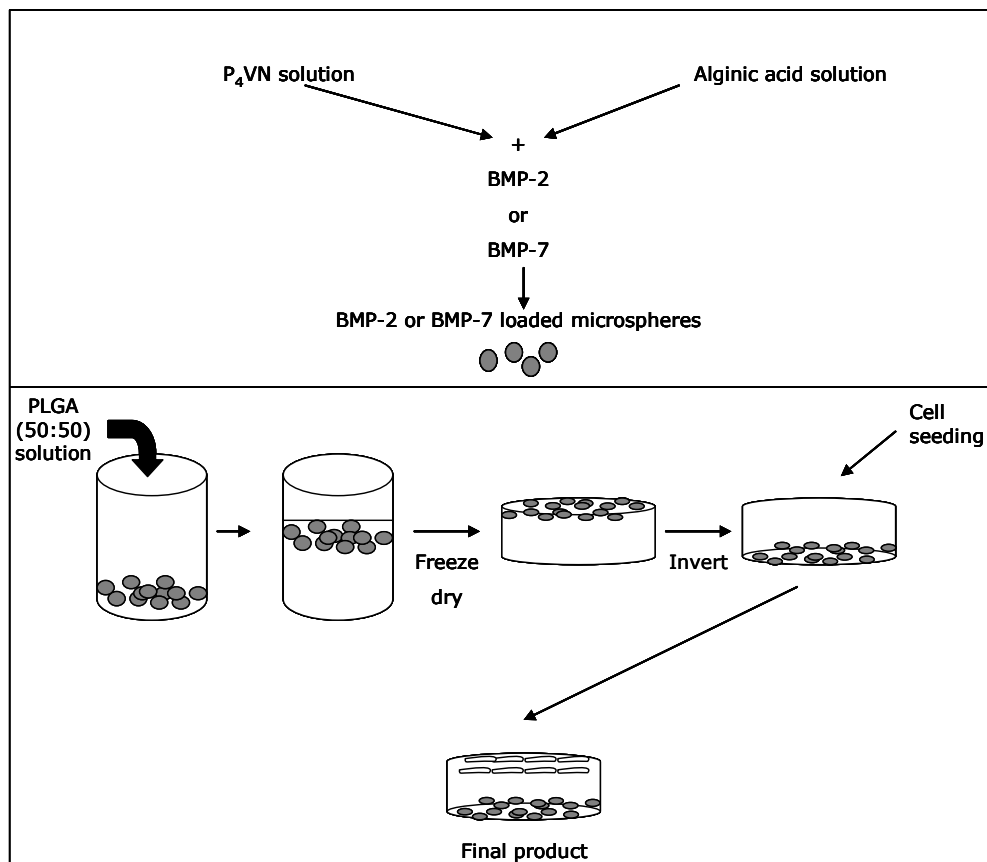


Figure 1. Schematic representation of the system designed.

CHAPTER 2

MATERIALS AND METHODS

2.1 Materials

Poly(4-vinylpyridine) (P₄VN) was purchased from Polysciences Inc. (USA). Poly(lactic acid-co-glycolic acid) (PLGA) (50:50) was purchased from Boehringer-Ingelheim (Germany). Bovine Serum Albumin (BSA) was purchased from Fluka Biochemica (Switzerland). Calcium chloride dihydrate was purchased from Riedel de Haën (Germany). Dioxane, ethanol and formaldehyde were purchased from Merck (Germany). Coomassie Plus - The better Bradford Assay™ Kit was purchased from Pierce (USA).

Cacodylic acid (sodium salt), glutaraldehyde (Grade I, 25 % aqueous solution), trypsin-EDTA (0.25 %), Amphotericin B, dimethyl sulfoxide (DMSO), Phalloidin, Trizma® Base, alginic acid, recombinant human Bone Morphogenetic Protein-2 (rhBMP-2) and recombinant human Bone Morphogenetic Protein-7 (rhBMP-7) were purchased from Sigma-Aldrich Co. (USA). Triton®X-100 was purchased from Applichem (USA). Dulbecco's Modified Eagle Medium (DMEM; high glucose) was purchased from Gibco (USA). Fetal calf serum (FCS) was purchased from PAA (Austria). Colorless DMEM (without sodium pyruvate and phenol red) was from HyClone® (USA). NucleoCounter reagents were purchased from Chemometec (Denmark). Alamar Blue was from Biosource (USA). Alkaline Phosphatase 307 Kit was purchased from Randox® (UK)

2.2 Methods

2.2.1 Preparation of P₄VN-Alginate-BSA Microspheres

Microspheres (ms) were prepared by internal gelation method [121,122] with CaCl₂ (3% w/v) as the crosslinker solution. P₄VN was dissolved in 1:1 dioxane/water. Alginate and BSA (the model protein) were dissolved together in distilled water. P₄VN and Alginate-BSA solutions were mixed in 3:1 volume ratio, respectively. The mixture was dropwise added to the mechanically stirred (Stir-Pak, Cole Parmer, USA) crosslinker solution using a 0.5 mL syringe and stirred for 1 h. After the crosslinking, the microspheres settled at the bottom of the beaker, the crosslinker solution was decanted and the microspheres were washed three times with dH₂O. After the removal of water the microspheres were frozen at -20 °C and freeze dried (FreeZone® 6 Liter Freeze Dry System, Labconco Co., USA) for 8 hours under 4.5x10⁻² mbar pressure.

In order to obtain different microsphere populations showing different release behaviors, certain parameters were investigated in the manufacturing process.

To determine the effect of polymer concentration on release behavior, microspheres were prepared with solutions with different concentrations of P₄VN and alginate (*Table 1*).

Table 1. Microsphere samples and their preparation conditions

Polymer concentration (%, w/v)	Preparation Solutions
4%	4% P ₄ VN, 4% Alginate
6%	6% P ₄ VN, 6% Alginate
8%	8% P ₄ VN, 8% Alginate
10%	10% P ₄ VN, 10% Alginate

In order to study the effect of crosslinking duration on release behavior, microspheres were prepared by crosslinking for 30 min and 1 h.

In order to study the effect of preparation temperature on release behavior, microspheres were prepared by crosslinking at 4°C and room temperature (RT).

2.2.2 Characterization of the Microsphere Populations

2.2.2.1 Stereomicroscopy of Microspheres

Stereomicrographs of freeze dried microspheres were obtained by Nikon SMZ 1500 (Japan).

2.2.2.2 Scanning Electron Microscopy of Microspheres

Microspheres were gold coated under vacuum and their micrographs were obtained by a Scanning Electron Microscope (SEM) (JSM 6400, JEOL, Japan) located in Metallurgical and Materials Engineering Department, METU.

2.2.3 Determination of Encapsulation Efficiency

To determine the amount of BSA entrapped in the microspheres, microBradford assay was performed.

Microspheres (2 mg) were partially dissolved in 1:1 EtOH/water solution. The solution was centrifuged the next day, at 10000 rpm for 10 minutes at +4°C (Sigma 3K30, Germany). The solvent was removed as supernatant and refreshed. After the removal of the supernatant EtOH was evaporated and the remaining sample was mixed thoroughly with Coomassie Plus™ Protein Assay Reagent in a 1:1 (v/v) ratio. The samples were incubated for 10 min at room temperature, then their absorbance at 595 nm was measured by UV-Visible spectrophotometer (Shimadzu 1201, Japan).

The amount of BSA was calculated from the calibration curve which was prepared within the theoretically calculated range of 0%-100% encapsulation (*Appendix A*). The procedure was repeated until no more BSA was detected in the solvent (4 times).

2.2.4 *In situ* Release Studies

Microspheres (4 mg) were incubated in 1 mL of PBS (0.01M, pH 7.4), the medium was removed and refreshed daily. The daily BSA release into the medium was determined by microBradford Assay as described (*Sec. 2.2.3*). The amount of BSA was calculated from the calibration curve (*Appendix B*). The release measurements were continued until no more BSA was detected in the release medium.

2.2.5 Preparation of PLGA Foams with Entrapped Microspheres

PLGA was dissolved in dioxane to yield a concentration of 4% (w/v). Microspheres were placed into glass containers of 1 cm diameter. PLGA solution (300 μ L) was poured into the containers. The mixture of PLGA solution and microspheres were frozen at -20 $^{\circ}$ C overnight and freeze dried the following day (FreeZone[®] 6 Liter Freeze Dry System, Labconco Co., USA) for 8 hours under 4.5×10^{-2} mbar pressure. Disc shaped foams with entrapped microspheres were obtained.

Samples prepared for characterization studies are listed in Table 2.

Table 2. Foam samples and their compositions

Sample Code	Composition
F	4 % PLGA foam
F-4	4 % PLGA foam + 5 mg 4% ms
F-10	4 % PLGA foam + 12 mg 10% ms
F-4&10	4 % PLGA foam + 5 mg 4% ms + 12 mg 10% ms

2.2.6 Characterization of Foams

2.2.6.1 Stereomicroscopy

Stereomicrographs of PLGA foams loaded with microspheres were obtained by Nikon SMZ 1500 (Japan).

2.2.6.2 Scanning Electron Microscopy

PLGA foams loaded with microspheres were gold coated under vacuum and their images were obtained by a Scanning Electron Microscope (SEM) (JSM 6400, JEOL, Japan) located in Metallurgical and Materials Engineering Department, METU.

2.2.6.3 Pore Size Distribution Analysis

The pore size distribution of PLGA scaffolds were determined by mercury porosimetry (PoreMaster 60, Quantachrome Corporation, USA) at METU Central Laboratory.

2.2.7 *In vitro* Studies

In vitro studies were performed with 4% and 10% microsphere populations containing the bone growth factors rhBMP-2 and rhBMP-7, respectively, instead of the model protein (BSA) used in the optimization studies. rhBMP-2 was lyophilized in dH₂O containing 0.1% BSA. BMP-7 was lyophilized in 4 mM HCl containing 0.1% BSA. Proper amounts of alginate were dissolved in the BMP solutions to yield a concentration of 4% for BMP-2 solution and 10% for BMP-7 solution. These solutions were then mixed with P₄VN solutions and turned into microspheres (see Sec. 2.2.1). Control groups were also prepared in a similar fashion but without growth factors. Samples prepared for use in *in vitro* studies are listed in Table 3.

Table 3. Microsphere loaded foams used in *in vitro* studies

Sample Code	Foam Type	BMP Content
F-2 (-)	F-4	-
F-2 (+)	F-4	BMP-2
F-7 (-)	F-10	-
F-7 (+)	F-10	BMP-7
F-2&7 (-)	F-4&10	-
F-2&7 (+)	F-4&10	BMP-2 + BMP-7

Teflon sheets were placed at the bottom of each well in 24 well plates to cover the polystyrene surfaces to avoid cell attachment. Disc shaped foams with microspheres were placed into the wells. UV sterilization was performed for 30 min in a laminar flow chamber (LaminAir Safe 2000, Holten A/S, Denmark).

2.2.7.1 Isolation of Rat Bone Marrow Stem Cells

Six week old, young adult, male, Sprague-Dawley rats weighing approximately 150 g were euthanized and disinfected with 1:1 (v/v) betadine-70% EtOH. Surgery took place in the laminar flow chamber under aseptic conditions.

The femur and tibia were excised and placed in 50 mL Falcon tube containing the harvest medium (10% Penicillin/Streptomycin (100 units/mL) in high glucose DMEM). Bones were then transferred to sterile petri plates with harvest medium. The femur and tibia were separated from each other by cutting from joints. The soft tissue covering the bones was removed and metaphyseal ends of the femur and tibia were cut off to enable access to the bone marrow in the midshaft. The needle of a sterile syringe containing 4 mL of primary medium (high glucose DMEM supplemented with 1% Penicillin/Streptomycin (100 units/mL) and 20% fetal calf serum (FCS)) was introduced to the femur and tibia midshafts, then the bone marrow was flushed out into 15 mL Falcon tubes.

The marrow cell suspensions in 15 Falcon tubes were centrifugated for 5 min at 3000 rpm (RotaFix 32, Hettich Zentrifugen, Germany). The supernatants which contained fatty cells were decanted and the remaining pellets were resuspended with 2 mL of primary medium by gently pipetting and breaking the clumps with 2 mL sterile pipettes. The cell suspensions were transferred to sterile T-75 tissue culture flasks and 8 mL of primary medium was added. T-75 flasks were placed into carbon dioxide incubator (5 % CO₂, Sanyo MCO-17AIC, Japan) at 37°C. The cultures were not disturbed for 2 days to enable cell attachment and proliferation. Then the medium was refreshed (high glucose DMEM supplemented with 1% Penicillin/Streptomycin (100 unit/ml) and 10% fetal calf serum (FCS)) every two days to remove unattached cells which were mainly red blood cells. After cells reached confluency, medium was discarded and washed with PBS (0.01M, pH 7.4) twice for complete removal of FCS since it is known to interfere with trypsin activity. Trypsin-EDTA solution (0.125%, PBS diluted from 0.25% stock) was added into the flasks and the cells were incubated for 2-3 min in the carbon dioxide incubator at 37°C until they detached from the polystyrene. Following detachment, medium was added into the flasks to terminate trypsin activity. The cell suspensions were centrifuged for 5 min at 3000 rpm. After the supernatant was discarded the cells were resuspended in FCS and counted with a Nucleocounter (Chemometec A/S Nucleo Counter, DENMARK). The cells in FCS were distributed to 2 mL cryovials for freezing. Cell number/vial did not exceed 1.10⁶ cells/mL. Dimethyl sulfoxide (DMSO) was added into cryovials to yield a concentration of 10%. Cryovials were placed into a freezing container (5100 Cryo 1°C Freezing Container, Nalgene, USA) which was then frozen at -70°C. The following day, cryovials were transferred to the liquid nitrogen tank (-196°C).

2.2.7.2 Culture of Bone Marrow Stem Cells

The frozen cells were taken out of the nitrogen tank and thawed quickly in hand until the DMSO liquidified. The suspension was poured into 15 mL DMEM medium (1% Penicillin/Streptomycin(100 unit/mL), 20% fetal calf serum, 0.4% Amphotericin B) and centrifuged at 3000 rpm for 5 min.

After the supernatant was discarded, the pellet was resuspended with 2.5 mL of DMEM medium. The resuspended cells were seeded onto T-25 polystyrene tissue culture flasks (TCPS) and were incubated for 1 week until they became confluent. The first medium change was made with 20% FCS containing DMEM and the following medium changes with 5% FCS containing DMEM.

2.2.7.3 Cell Seeding on Foams

The medium in the flasks was discarded and 1.5 mL of 0.125 % trypsin-EDTA was added into each flask. The cells were incubated in trypsin for 4-5 min. After their detachment was observed with the light microscope, the trypsin-cell mixture was transferred into 2 mL of DMEM medium in order to stop trypsin activity. The cells were centrifuged at 3000 rpm for 5 min, the supernatant was discarded and the cells were resuspended in 2 mL of high glucose DMEM (1% Penicillin/Streptomycin(100 unit/ml), 10% FCS, 0.4% Amphotericin B). The number of viable cells was quantified by using the Nucleocounter then 4×10^4 cells were seeded onto each foam sample. The samples were incubated at 37°C for 1 h for attachment onto the foam. After 1 h, 1.2 mL of medium was added onto each well. Cell medium was changed every three days.

2.2.7.4 Cell Proliferation Assay

2.2.7.4.1 Alamar Blue Optimization for BMSc

In order to investigate cell proliferation, Alamar Blue assay was performed. Alamar Blue calibration curve was prepared for BMSCs cultured with DMEM until confluency. Following the trypsinization and cell counting (see Sec. 2.2.7.3), cell seeding on 24 well plate was performed with differing cell numbers between (2×10^4 and 3×10^5) on different wells. The cells were incubated for 3 h for attachment on the TCPS. After 3 h, the medium was removed and 1.2 mL Alamar Blue solution (10% in colorless DMEM medium) was added into each well and the cells were incubated for 1 h in Alamar Blue solution.

After 1 h, 200 μ L of the Alamar Blue solution from each well was removed and added into a 96 well tissue culture plate and their absorbance was measured at 595 nm and 570 nm by the Elisa Plate Reader (Maxline Vmax®, Molecular Devices, USA).

Percent reduction of the dye due to the metabolic activity of the cells was determined by using absorption coefficients of the reduced and oxidized dye. Calibration curve was constructed as the reduction percentage versus cell number (*Appendix C*).

2.2.7.4.2 Cell Proliferation

The medium in cell seeded PLGA foams was removed and the wells were washed with colorless DMEM medium (1% Penicillin/Streptomycin (100 unit/mL)) 3 times until the color of the DMEM was eliminated. Alamar Blue solution (1.2 mL, 10% in colorless DMEM medium) was added onto each well and the cells were incubated for 1 h with Alamar Blue solution in CO₂ incubator. After 1 h, 200 μ L of the Alamar Blue solution from each well was added into a 96 well tissue culture plate and their absorbance was measured at 595 nm and 570 nm by the Elisa Plater Reader (readings were performed in triplicate). The wells were washed with colorless DMEM medium (1% Penicillin/Streptomycin) 3 times until the color of the Alamar Blue was removed to a high extent, then 1.2 mL of medium was added onto each well for continuity of culture.

The absorbance values were analyzed according to the previously prepared calibration curve for BMSCs (*Appendix C*). Alamar Blue testing was performed on Day 7, 14 and 21 of culturing. Unseeded foams kept under the same culture conditions for each group were used as blank samples.

2.2.7.5 Determination of Cell Differentiation by ALP Assay

Alkaline phosphatase (ALP) assay was performed for cell seeded PLGA foams cultured for 7, 14 and 21 days. At these time points, the medium of the PLGA foams was removed, the foams were washed with PBS twice and transferred into 700 μL of Tris Buffer (10mM, pH 7.5, 0.1% Triton[®]X-100) containing 15 mL Falcon tubes and stored at -20°C until the assay was performed. On the day of the assay, foams in the lysis buffer were thawed in the CO_2 incubator at 37°C and then frozen at -20°C to ensure complete lysis and this cycle was repeated three times. Then each sample was sonicated for 5 min at 25 W (Ultrasonic Homogenizer, Cole Parmer, USA) in ice. Sonication was performed in 30 on, 30 off cycles, in total for 10 minutes. The samples were then centrifuged at 2000 rpm for 10 min. 100 μL of each supernatant was added to 150 μL of substrate (p-nitrophenyl phosphate reconstituted with MgCl_2 -diethanolamine buffer supplied by Randox AP307 kit). The time dependent absorbance of the mixture was obtained at 405 nm every 2 min for a total of fourteen min by Elisa Plate Reader (readings were performed in duplicate). OD_{405} vs. time graph of each sample was drawn and the slopes were calculated. The data was analyzed by using the slope of the calibration curve previously prepared with p-nitrophenol (*Appendix D*) to determine enzyme activity in units of nmol substrate converted to product/min.

ALP activity (nmoles/min/sample) was calculated as follows:

$$\text{Net OD}_{405} = \text{OD}_{405, \text{ seeded foam}} - \text{OD}_{405, \text{ unseeded foam}}$$

$$\text{Slope of Net OD}_{405} \text{ vs. Time graph} = \text{Net OD}_{405} / \text{min for sample}$$

$$\text{Slope of calibration curve} = \text{OD}_{405} / \text{nmoles of p-nitrophenol}$$

$$\text{ALP Activity (nmoles/min/sample)} = [(\text{Net OD}_{405} / \text{min for sample}) / (\text{OD}_{405} / \text{nmoles of p-nitrophenol})] \times (\text{Total volume of lysis buffer } (\mu\text{L}) / \text{Amount added on the substrate } (\mu\text{L}))$$

2.2.7.6 Phalloidin Staining

On day 21 of the culture, cells were fixed with formaldehyde (4% formaldehyde in PBS) for 30 min. After fixation, foams were washed with PBS (0.01M, pH 7.4) three times for 3-4 min. Then the cell membranes were incubated in 1% Triton X-100 for 5 min at room temperature to permeabilize the cell membranes to enable dye penetration. Following permeabilization, samples were washed with PBS several times to remove Triton X-100 and were incubated in 1% BSA containing PBS solution at 37°C for 30 min in order to block the non-specific binding sites. The samples were washed with PBS and incubated for another 1 h at 37°C in FITC labeled Phalloidin (0.5 µg/ml FITC-labelled Phalloidin in 0.1% PBS-BSA) for staining the cytoskeletal filamentous actin (F Actin). Finally, the samples were washed with PBS, transferred to a microscope slide and examined with confocal microscope (Leica DM2500, Leica Microsystems, Germany) with the filter for excitation at 488 nm.

2.2.7.7 SEM images of Cell Cultured Foams

On day 21 of culture, cells were fixed with glutaraldehyde (2.5% glutaraldehyde in 0.1M, pH 7.4 sodium cacodylate buffer) for 2 h. After fixation, they were washed with cacodylate buffer three times. The samples were frozen at -20°C and freeze dried the following day, for 8 h under 4.5×10^{-2} mbar pressure. The dry samples were gold coated under vacuum and then visualized by Scanning Electron microscope (SEM) (JSM 6400, JEOL, Japan) located in Metallurgical and Materials Engineering Department, METU.

CHAPTER 3

RESULTS AND DISCUSSION

3.1 *In situ* Release Profiles of P₄VN-BSA-Alginate Microspheres

Microspheres constructed by complexation of P₄VN and alginate entrapping the model protein BSA, were tested *in situ* for their release behavior. A kinetic model for the release behavior was sought.

3.1.1 Influence of Polymer Concentration on Release Behavior

In order to obtain two microsphere populations to use in sequential release of proteins, and especially of growth factors, microspheres of different polymer concentrations were prepared and their *in situ* release profiles were obtained by microBradford assay (Fig. 2).

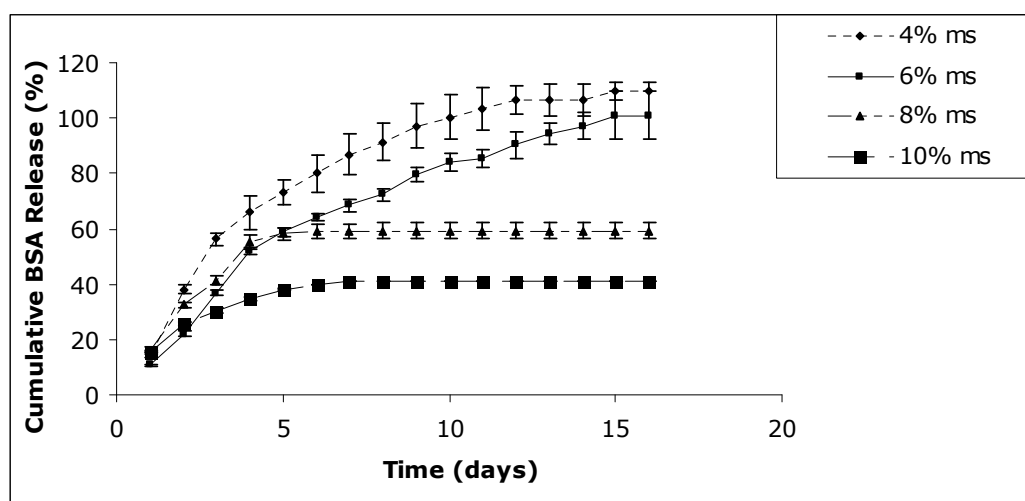


Figure 2. Influence of polymer concentration on BSA release from 4%, 6%, 8% and 10% microspheres.

An initial burst effect with the release of large fraction of total BSA content in the first few days was observed for all types of microspheres. The 4%, 6%, 8% and 10% microspheres released 56%, 37%, 41% and 30% of their content, respectively, by day 3 (*Fig. 2*). This was followed by a much lower BSA release for all types of microspheres. The 4% and 6% microspheres released all of their content in 10 and 15 days, respectively. The 8% and 10% microspheres, on the other hand released only 59% and 41% of their content, respectively, in 7 days. No release from the latter two was detected in the following 9 days during which the study was continued. This could be due to increased retention of BSA in denser matrices of microspheres prepared using higher polymer concentrations and low amount of BSA released daily being below the sensitivity limit of the microBradford assay (1 µg/mL). A recent study which reported detection of BSA release from highly crosslinked, dense chitosan microspheres only after 24 days of incubation due to very low or delayed release supports this conclusion [133].

Release from pure alginate beads is generally completed within hours [134]. Therefore, complexation of alginate with other polymers, mostly polycations is required for strengthening these particles and prolonging the release behavior [135]. For instance, release duration has been shown to be extended from 6 h to 4 days when alginate was complexed with chitosan. On the other hand, duration was extended only to 30 h when poly(L-lysine) was administered as the polycation [136]. These findings clearly demonstrate that extension of release duration by polyelectrolyte complexation is also dependent on the type of the polyelectrolyte molecule utilized. Results obtained in this study are very promising in terms of achieving prolonged release through complexation of alginate with P₄VN.

The kinetic analysis of the release behavior was made by trying to fit the data to release relations for Higuchi, Zero Order and First Order release kinetics. The results are presented in Table 4.

For Zero Order release model, M_t vs t was plotted according to Equation 1:

$$M_t/M = k_0 t \quad (1)$$

For First Order release model, $\ln M_t$ vs t was plotted according to Equation 2:

$$M_t = M e^{k_1 t} \quad (2)$$

For Higuchi release model, M_t/M vs $t^{1/2}$ was plotted according to Equation 3:

$$M_t/M = k_H t^{1/2} \quad (3)$$

where; M_t and M are the amount of protein released at time t (days) and at time infinity, respectively, t is time (days) and k_0 , k_1 and k_H are rate constants for Zero Order, First Order and Higuchi release models, respectively.

In all the cases, in order to claim fit, the data points need to fall on a straight line yielding the slope k . An example of kinetic analysis of data for 4% microspheres (crosslinked for 1 h at RT) in accordance with Higuchi model is given in Figure 3.

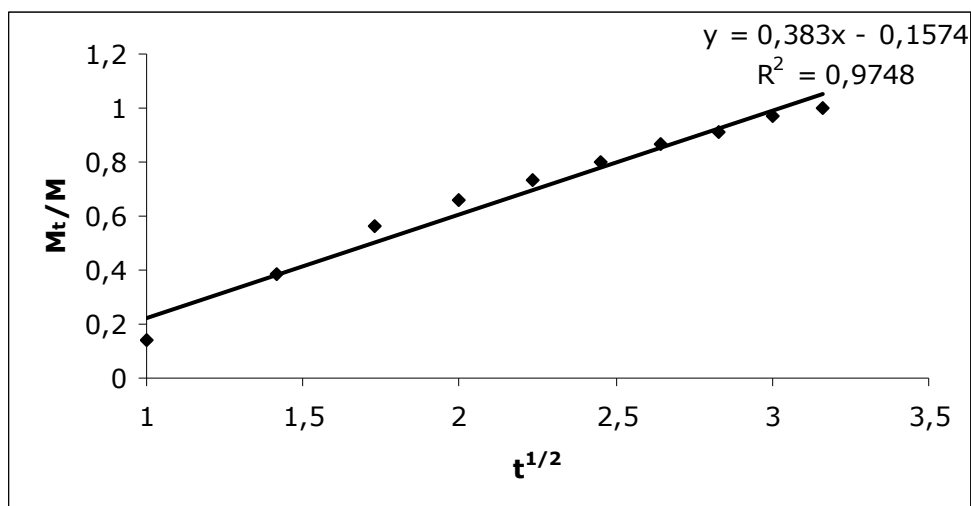


Figure 3. Kinetic analysis of 4% microspheres in accordance with Higuchi release model.

Table 4. Kinetic analysis of release from microspheres of different polymer concentrations

Polymer Concentration (% w/v)	Release Models and Release Parameters (k and r ²)					
	Zero Order		First Order		Higuchi	
	k ₀	r ²	k ₁	r ²	k _H	r ²
4	0.0866	0.9106	0.1656	0.7155	0.383	0.9748
6	0.0617	0.9247	0.1291	0.7306	0.314	0.9827
8	0.0873	0.9038	0.2438	0.8191	0.312	0.9556
10	0.0404	0.9097	0.1439	0.8209	0.154	0.9698

The best fits (highest r² values) were obtained with the Higuchi model for each of the microsphere populations indicating that the release from the polyelectrolyte complex microspheres of P₄VN and alginic acid is diffusion controlled (*Table 4*).

As expected, k_H values showed that release rate decreases with increasing polymer concentration. There are two main reasons for slower release rates with increased polymer concentrations. As the polymer concentration of the preparation medium increases, the polymer matrices in the resultant microspheres become denser yielding more tortuous diffusion pathways, and therefore, slower release rates [134, 137]. Another factor governing the rate of release from microspheres is the particle size. It was observed in this study that the particle size increased with increase in polymer concentration (*Fig. 6*). The surface area/volume ratio is lower and diffusion path length is higher in the larger microspheres thus yielding slower release rates [138].

Based on the release profiles and highest release rates obtained 4% microspheres were selected as the early stage component. 10% microspheres were selected as the long term release component because of their release rate being the lowest.

3.1.2 Influence of Crosslinking Duration on Release Behavior

The influence of the duration of crosslinking of alginate with calcium ions on *in situ* release behavior was investigated for 4% and 10% microspheres subjected to 30 min and 1 h of crosslinking (Fig. 4) and the data was treated in accordance with the Higuchi model and presented in Table 5.

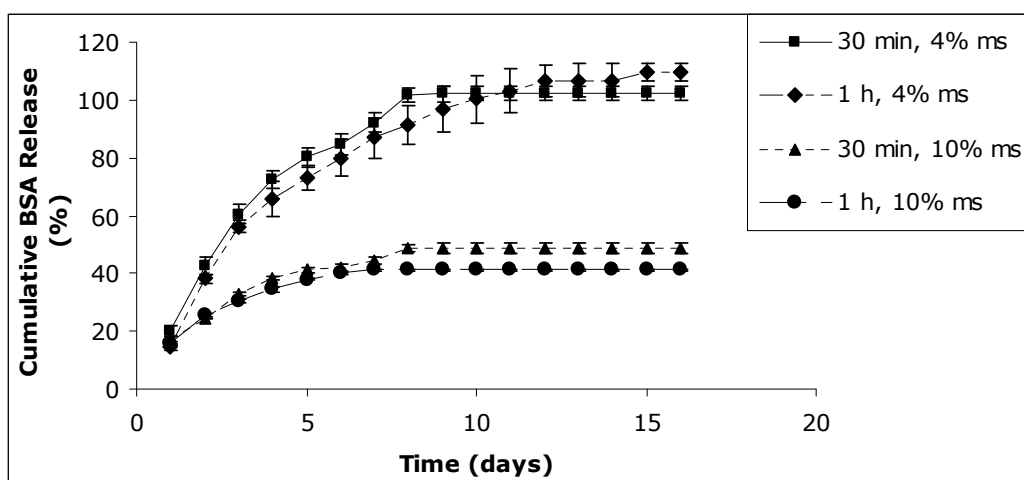


Figure 4. Influence of crosslinking duration on BSA release from 4% and 10% microspheres.

Release profiles demonstrated that, 30 min crosslinked 4% microspheres released 61% of their content by day 3 whereas this number was slightly reduced to 56% with an additional 30 min of crosslinking duration (Fig. 4). Increase in crosslinking duration generated a lesser reduction (from 32% to 30%) in the release from 10% microspheres by day 3. Duration of release was not extended by altering crosslinking duration in either of the microsphere populations. These values do not support the expectation that increasing crosslinking duration prolongs release. This is not in accordance with the previously reported alginate beads [139].

Table 5. Kinetic analysis of release from microspheres with different crosslinking durations

Polymer Concentration (% w/v) and Crosslinking Duration (min)	Release Parameters According to Higuchi Model (k_H and r^2)	
	k_H	r^2
4, 30	0.427	0.9835
4, 60	0.383	0.9748
10, 30	0.167	0.9687
10, 60	0.154	0.9698

The kinetic data in this study also confirmed that release rates did not change significantly by change in crosslinking duration (*Table 5*). However, the rate and mechanism of crosslinking is the determinant here. If the crosslinking is very rapid, by 30 min it is possible that the reaction is already over thus no further change could be detected upon prolonging the crosslinking duration.

Since obtaining microspheres with prolonged release was one of the main objectives of this study, 1 h crosslinking duration was used in the rest of the study even though the improvement was slight. However, this duration was not increased further to avoid the loss of BSA by leakage into the aqueous solution during crosslinking leading to low encapsulation efficiencies (*Sec. 3.2.1*).

3.1.3 Influence of Crosslinking Temperature on Release Behavior

The influence of crosslinking temperature on *in situ* release behavior was investigated for 4% and 10% microspheres crosslinked at 4°C and room temperature (*Fig. 5*). The release data was treated in accordance with the Higuchi model and presented in *Table 6*.

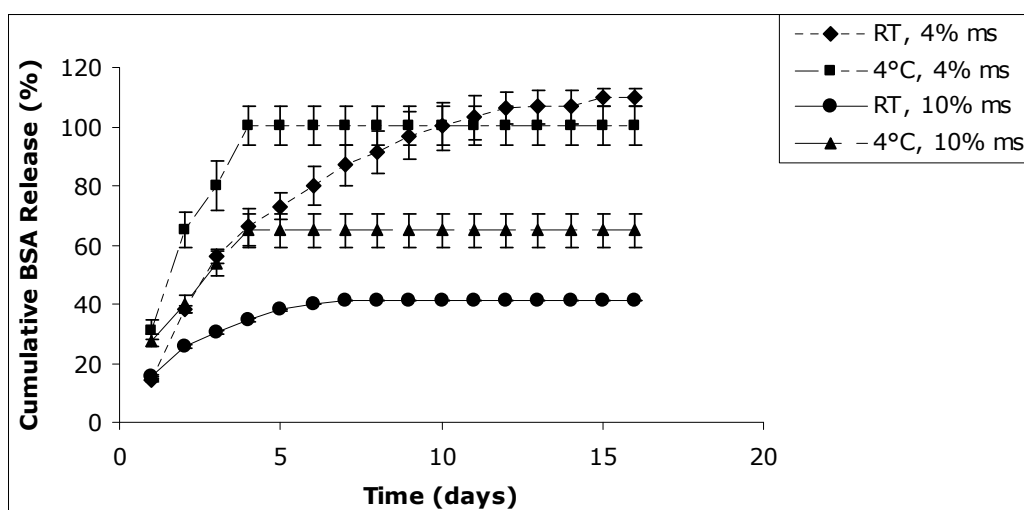


Figure 5. Influence of crosslinking temperature on BSA release from 4% and 10% microspheres.

A significant difference was observed in release profiles of microspheres prepared at 2 different crosslinking temperatures, especially in the first 5 days and until 30-70% of the content was released. 4% microspheres crosslinked at 4°C released all of their content in 4 days whereas this period was 10 days for 4% microspheres crosslinked at RT. 10% microspheres released 65% of their content in 4 days whereas 10% microspheres crosslinked at RT released only 35% of their content in the same period (*Fig. 5*).

Table 6. Kinetic analysis of release from microspheres with different crosslinking temperatures

Polymer Concentration (% w/w), Crosslinking Temperature (°C)	Release Parameters According to Higuchi Model (k_H and r^2)	
	k_H	r^2
4, 25	0.672	0.9748
4, 4	0.383	0.9891
10, 25	0.375	0.9698
10, 4	0.154	0.9922

Kinetic data suggests that there is an approximately 2 fold increase in release rates when crosslinking temperature is reduced to 4°C (*Table 6*). This difference can be attributed to slower crosslinking and solidification due to a decrease in the crosslink degree of microspheres at lower temperatures. Another possibility is that entrapment is less efficient due to molecules (P₄VN and alginate) being more compact and less mobile at the lower temperature leading to a faster loss of content, BSA.

Preparation of microspheres at 4°C has yielded high release rates and unfavorable release durations limited to a few days, therefore, crosslinking temperature in the rest of the study was set as room temperature.

3.2 BSA Entrapment Efficiency of P₄VN-Alginate Microspheres

3.2.1 Influence of Polymer Concentration on Entrapment Efficiency

Entrapment efficiencies of microspheres of different polymer concentrations were investigated by repetitive extraction through dissolution of microspheres in EtOH/water (1:1, v/v) solution (*Table 7*). Entrapment efficiency was calculated as ratio of BSA entrapped in microspheres to the amount of BSA in the loading medium (% w/w).

Table 7. Effect of polymer concentration on entrapment efficiency

Polymer Concentration (%, w/v)	Entrapment Efficiency (%)
4	9.31 ± 1.92
6	8.07 ± 1.80
8	5.25 ± 0.73
10	6.92 ± 0.75

The entrapment efficiencies of 5-10% for all types of microspheres prepared in this study were low (*Table 7*) when compared to some studies which involved polyelectrolyte complexes [140]. However, some other studies reported similar low entrapment efficiencies such as in the case of chitosan-alginate microspheres with insulin entrapment efficiency of 11% [141] or 3.5-11.4% entrapment efficiency of alginate beads prepared by internal gelation [142]. Entrapment efficiency is highly dependent on the preparation methods. For instance, the main disadvantage of using internal gelation is the loss of protein during the crosslinking due to escape of the protein through the pores [135]. This can be a major limitation especially with water soluble proteins. The wash step following crosslinking is also believed to contribute to the loss of some of the entrapped protein. It has been reported that protein loss of up to 35% can occur during this step [138]. Another study reported decrease of entrapment efficiency from 69% to 8% due to extraction of the hydrophilic drug at the washing steps [143].

Another reason for the low entrapment efficiency could be experimental. When polyelectrolyte complexes are crosslinked, they become so strong that they do not dissolve even in the presence of Ca^{+2} chelating agents [144]. As already stated in section 2.2.3, microsphere dissolution was partial in EtOH/water (1:1, v/v) solution. It is possible that low efficiencies could result from incomplete extraction of BSA with the EtOH/water (1:1, v/v) solution. Another reason for incomplete extraction could be the interaction between the polyelectrolytes and BSA. BSA (pI 4.8) possesses a negative charge at neutral media [145]; therefore, it is possible that strong interactions between P₄VN and BSA prevented complete removal of BSA from the partially dissolved polymer network since it is known that polyelectrolytes can strongly bind to proteins [146].

3.2.2 Influence of Crosslinking Duration on Entrapment Efficiency

Entrapment efficiencies of 4% and 10% microspheres subjected to 30 min and 1 h crosslinking are presented in Table 8.

Table 8. Effect of polymer concentration and crosslinking duration on entrapment efficiency

Polymer Concentration (% w/v)	Entrapment Efficiency (% w/w)	
	Crosslinking Duration (min)	
	30	60
4	11.07 ± 0.29	9.31 ± 1.92
10	7.66 ± 0.21	6.92 ± 0.75

A decrease in entrapment efficiency with increase in crosslinking duration was observed (*Table 8*). Thus an expected increase in entrapment efficiency does not result when the duration is increased implying that crosslinking is quite complete within the first 30 min and the following 30 min simply leads to the leakage of the entrapped material.

A decrease in entrapment efficiency was also observed with an increase in polymer concentration. As polymer concentration increased from 4% to 10%, decrease from 11% to 8% and from 9% to 7% was observed for microspheres crosslinked for different durations (*Table 8*). This issue about the influence of polymer concentration on entrapment efficiency is quite controversial. The entrapment efficiency was reported to increase from 69% to 86% with increase of polymer concentration from 2% to 8% in PLGA microparticles [147]. In contrast, it was reported that efficiency of BSA entrapment by chitosan (polycation)-tripolyphosphate (polyanion) nanoparticles decreased from 88% to 61% with an increase of chitosan concentration from 1% to 3% (w/v) [148]. Another study reported that, although increasing chitosan concentration up to 0.75% resulted in an increase in BSA entrapment efficiency of chitosan-alginate microcapsules, entrapment was extremely difficult above 0.75% (w/v) due to increased viscosity [149]. Therefore, observations in this study were attributed to the increased viscosity of the polymer solutions which complicated entrapment in the structure. The increased polymer concentration also changed the morphology of the microspheres (*Fig. 6, Fig. 7*). This could be another reason for decrease in entrapment efficiency.

3.2.3 Influence of Crosslinking Temperature on Entrapment Efficiency

Entrapment efficiencies of 4% and 10% microspheres crosslinked at RT and 4°C were investigated (*Table 9*).

Table 9. Effect of crosslinking temperature on entrapment efficiency

Polymer Concentration (% w/v)	Entrapment Efficiency (% w/w)	
	Crosslinking Temperature (°C)	
	4°C	25
4	1.74 ± 0.21	9.31 ± 1.92
10	2.53 ± 0.14	6.92 ± 0.75

The entrapment efficiencies for both types of microspheres decreased significantly when crosslinking temperature was decreased to 4°C (*Table 9*). This could be due to slower, and therefore, insufficient crosslinking of microspheres at lower temperatures which would consequently ease escape of BSA to the crosslinker solution during production.

3.3 Microscopy of Microsphere Populations

3.3.1 Stereomicroscopy

Stereomicrographs of 4% and 10% microspheres were obtained following freeze drying (*Fig. 6*).

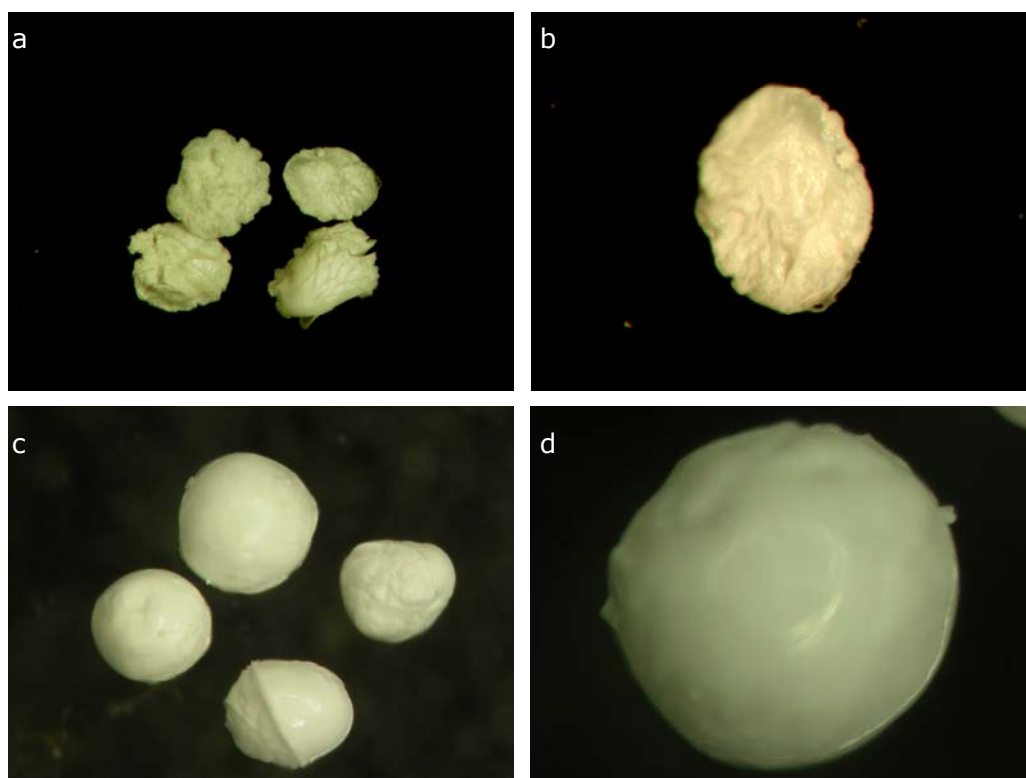


Figure 6. Stereomicrographs of microspheres. (a) 4% (x 12), (b) 4% (x 30), (c) 10% (x 12), d) 10% (x 30).

The microsphere sizes were observed to increase with increase in polymer concentration (*Fig. 6*). This increase was a result of the presence of higher amounts of polymer in the droplets increasing their viscosity [138].

As a result of these two factors larger droplets were formed when polymer concentration was higher. The spherical shapes of microspheres were lost following freeze drying. This was especially obvious with 4% microspheres. These observations are consistent with previously reported drying due shape loss of Ca^{+2} crosslinked alginate-polycation beads [150]. The 4% microspheres had rougher and more wrinkled surfaces (*Fig. 6 a, b*) when compared to 10% microspheres (*Fig. 6 c, d*). This was due to increased density of the microspheres caused by the increase in the polymer concentration and is consistent with the literature [134].

3.3.2 Scanning Electron Microscopy

SEM images of 4% and 10% microspheres were obtained following freeze drying (*Fig. 7*).

The pore diameter of alginate microspheres were reported to be between 5-200 nm [135]. The SEM images of 4% microspheres (*Fig. 7 a, b*) are typical [136]. However, pore sizes of 10% microspheres on the surface are close to 5 μm (*Fig. 7 c, d*). This could be due to lowered crosslink density of 10% ms with lowered Ca^{+2} /alginate ratio since concentration and volume of CaCl_2 solution was constant whereas polymer concentration increased 2.5 fold for 10% ms. It is also known that increasing Ca^{+2} /alginate ratio increases degree of shrinkage [151]. Reduced pore sizes due to higher shrinkage can explain the difference in pore sizes between 4% and 10% microspheres. This observation can also be due to excessive shrinkage of the low polymer concentration microspheres appearing falsely smooth upon collapsing during freezing or drying.

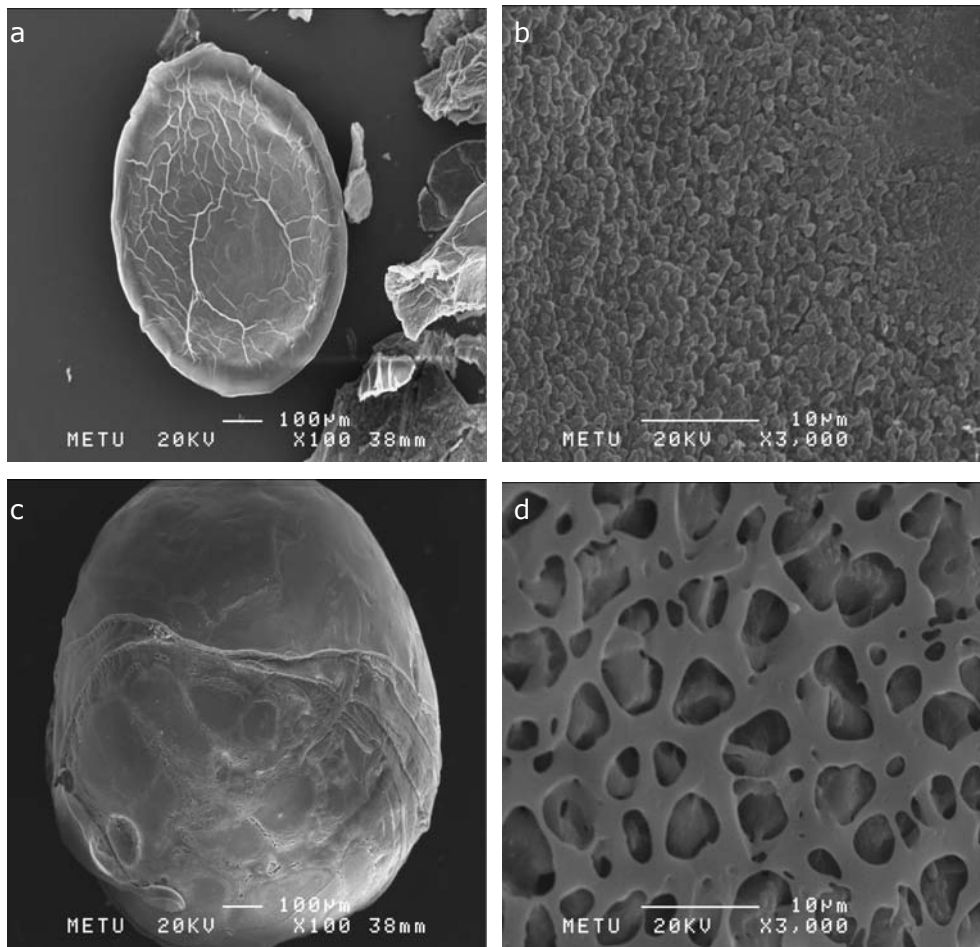


Figure 7. SEM images of microspheres. (a) 4% (x 100), (b) 4% (x 3000), (c) 10% (x 100), (d) 10% (x 3000).

3.4. Microscopy of Foams

3.4.1 Stereomicroscopy

Cell seeding surfaces and microsphere-foam interfaces of microsphere containing foams (*Table 2*) were visualized by Nikon SMZ 150 (*Fig.8*).

Disk shaped foams had a diameter of 1 cm and a thickness of 0.4 cm. The thickness was lesser in the center, approximately 0.1 cm for F-4 and F-10 and 0.2 cm for F-4&10.

The microspheres were located on the top side of the foams, due to floating of microspheres to surface after PLGA solution (4%, w/v, in dioxane) was introduced to the cylindrical glass molds. After preparation, the disks were turned over and cell seeding was made on the side where microspheres were not located (*Fig. 8 a*) in order to maximize PLGA-cell contact.

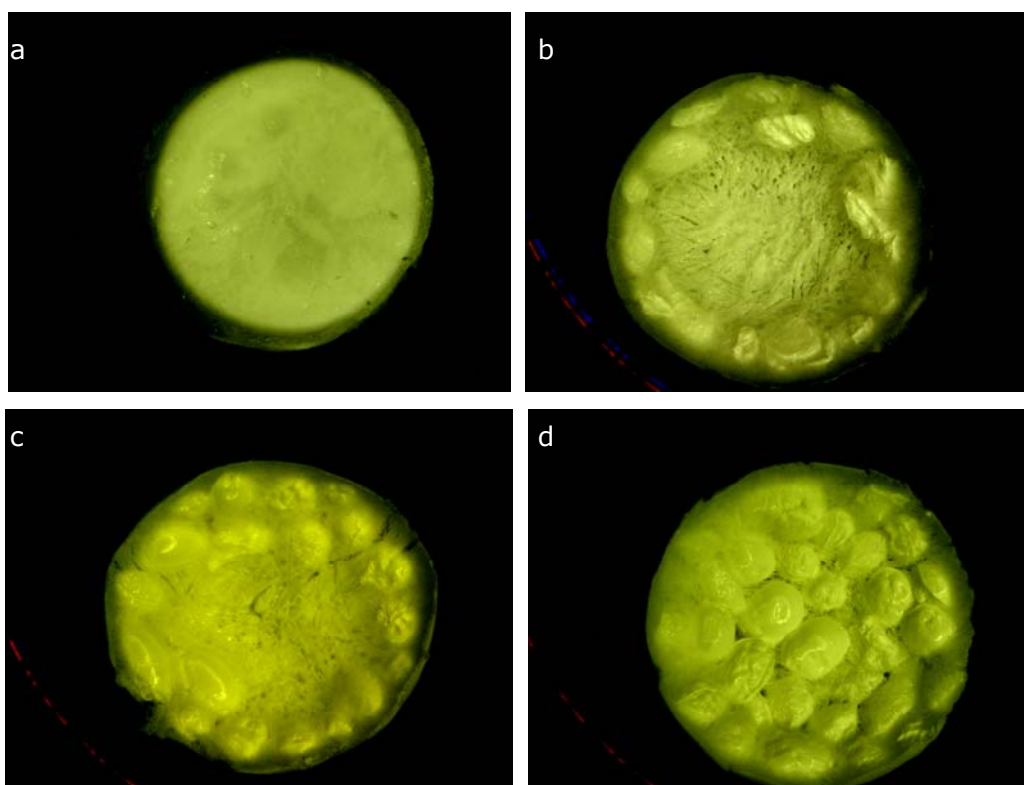


Figure 8. Stereomicroscope images of PLGA foams with microspheres. (a) Cell seeding surface, (b) F-4 bottom, (c) F-10 bottom, (d) F-4&10 bottom. Original magnification: x 2.25.

3.4.2 Scanning Electron Microscopy

SEM images of cell seeding surfaces and microsphere-foam interfaces of microsphere containing foams are presented in Fig. 9.

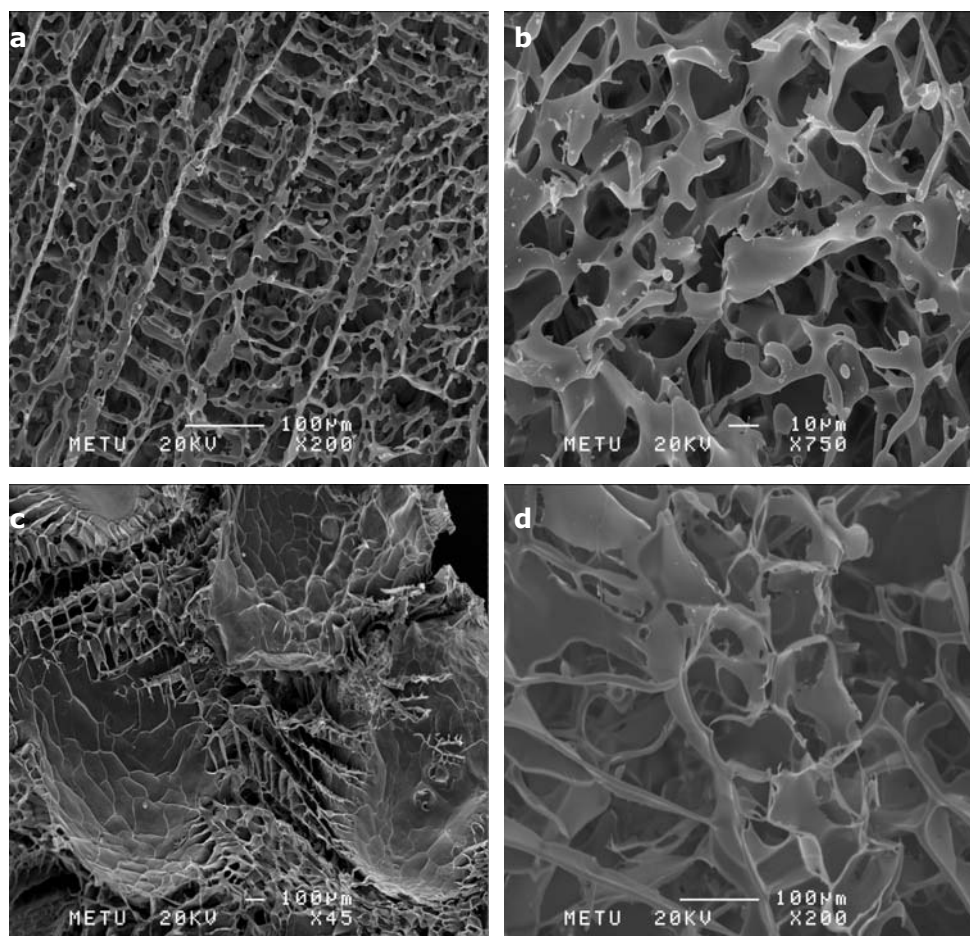


Figure 9. SEM images of PLGA foams with microspheres (a) Cell seeding surface, (x 200), (b) cell seeding surface, (x 750), (c) foam-microsphere interface, (x 45), (d) foam-microsphere interface, (x 200).

SEM images have revealed the highly porous nature of foams (*Fig. 9 a, b, d*) and entrapment of microspheres in foam structures (*Fig. 9 c*).

3.5 Pore Size Distribution Analysis of Foams with Microspheres

Pore size distribution analysis of F, F-4, F-10 and F-4&10 (Table 2) was performed by Mercury Porosimetry (Fig. 10).

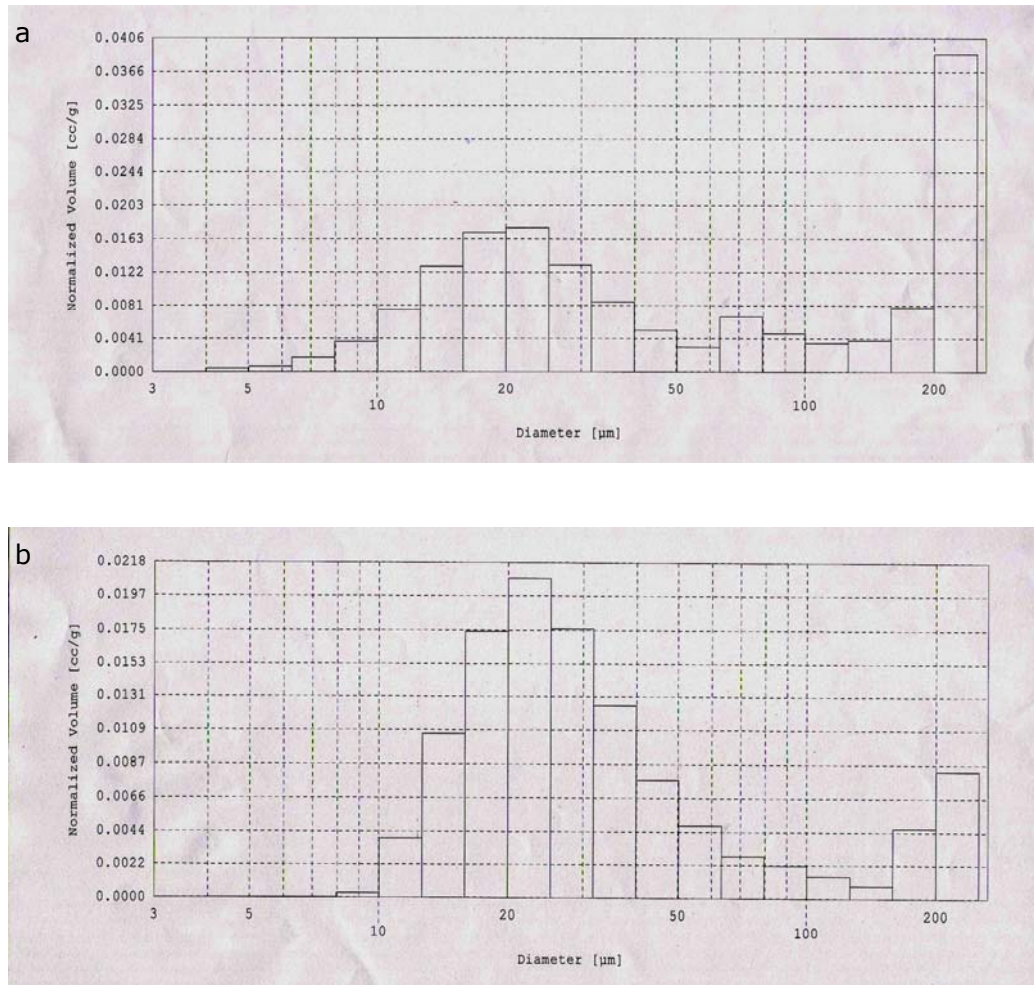


Figure 10. Pore size distribution of foams (a) F, (b) F-4, (c) F-10, (d) F-4&10.

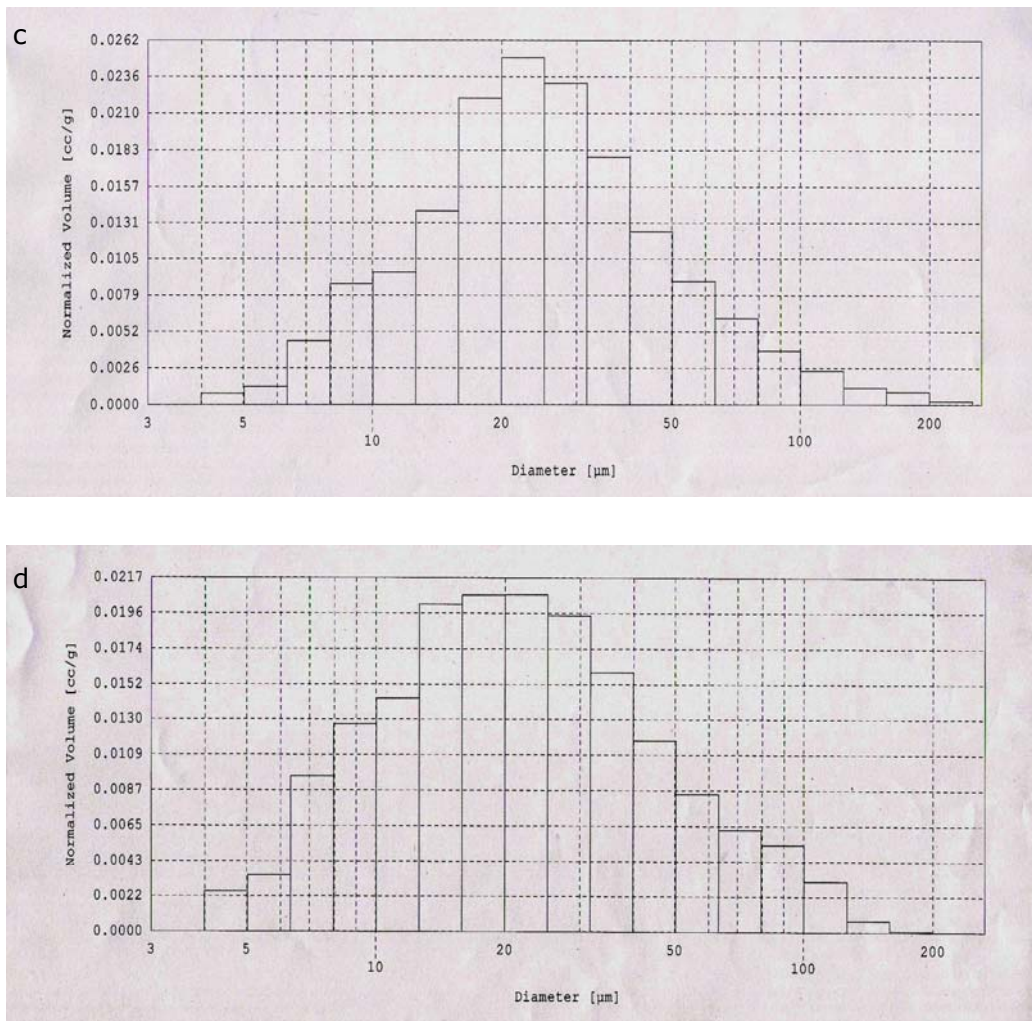


Figure 10. cont'd

In general, the highest fraction of the pores had a diameter around 20 μm . A significant difference in terms of pore size distribution was observed with entrapment of porous microspheres in the foam structure. Pores larger than 200 μm constituted a significant fraction in the microsphere free foam (Fig. 10 a). This volume was reduced to a great degree upon introduction of microspheres into the foam (Fig. 10 b, c, d). Although F-4 still contained pores larger than 200 μm (Fig. 10 b), F-10 (Fig. 10 c) and F-4&10 (Fig. 10 d) had none. On the contrary, volume fraction of pores with diameters between 10-50 μm and below 10 μm was significantly higher in F-4&10 in comparison to F-4 and F-10 (F-4 contained almost no pores below 10 μm).

It was reported that pore sizes smaller than 10 μm are important in cell proliferation [16]. Therefore, the differences between F4&10 and the other two in terms of volume occupied by pores smaller than 10 μm was expected to have an influence on cell proliferation in this study.

3.6 In vitro Studies

3.6.1 Cell Proliferation

Cell proliferation was determined by Alamar Blue assay on the 7th, 14th and 21st days of culture.

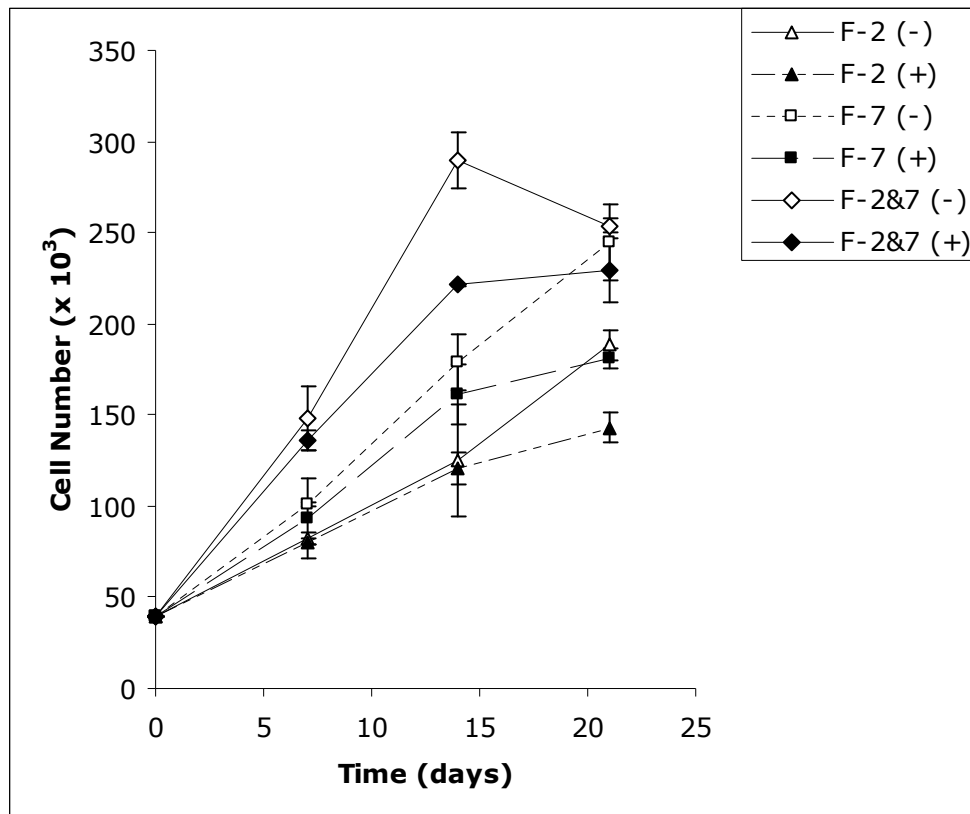


Figure 11. Cell proliferation curves in BMP (+) and BMP (-) foams.

In general, there was an increase in cell numbers throughout the 21 day culture, with the only exception of F-2&7 (-) which showed a significant decrease between days 14 and 21, probably due to cell death with overpopulation of foams by cells (*Fig. 11*). Proliferation of cells on F-2&7 foams was higher regardless of BMP presence at all times in comparison to F-2 and F-7 (with the exception of cell numbers of F-2&7 (-) and F-2&7 (+) being very close to F-7 (-) on day 21). The difference was greatest on day 14. This can be attributed to different physical characteristics of F-2&7, such as pore size distribution (*Fig. 10*). According to this data it can be suggested that regardless of BMP presence, F-2&7 was the most efficient foam type in terms of positive proliferative influence. F-2&7 was followed by F-7 and F-2, respectively (*Fig. 11*). These findings could be explained by the observation that microporosity, which is known to be important in proliferation [16], was highest in F-2&7 and was followed by F-7 and F-2, respectively (*Fig. 10*).

Interestingly, BMP (-) groups had at all times more cells than their corresponding BMP containing counter parts (*Fig. 11*); this implied a suppression by BMPs. It is known that osteogenic activity increases with down regulation of cell proliferation [152]. The cell number of F-2&7 (+) was significantly lower than F-2&7 (-) on day 14. Similar observation was made for F-2 (+) and F-7 (+) at the later date (day 21). These imply increased osteogenic activity by BMP carrying foams and the effect was observed earlier in the case of double BMP carrying F-2&7 (+).

3.6.2 ALP Activity

ALP activity was determined on the 7th, 14th and 21st days of culture.

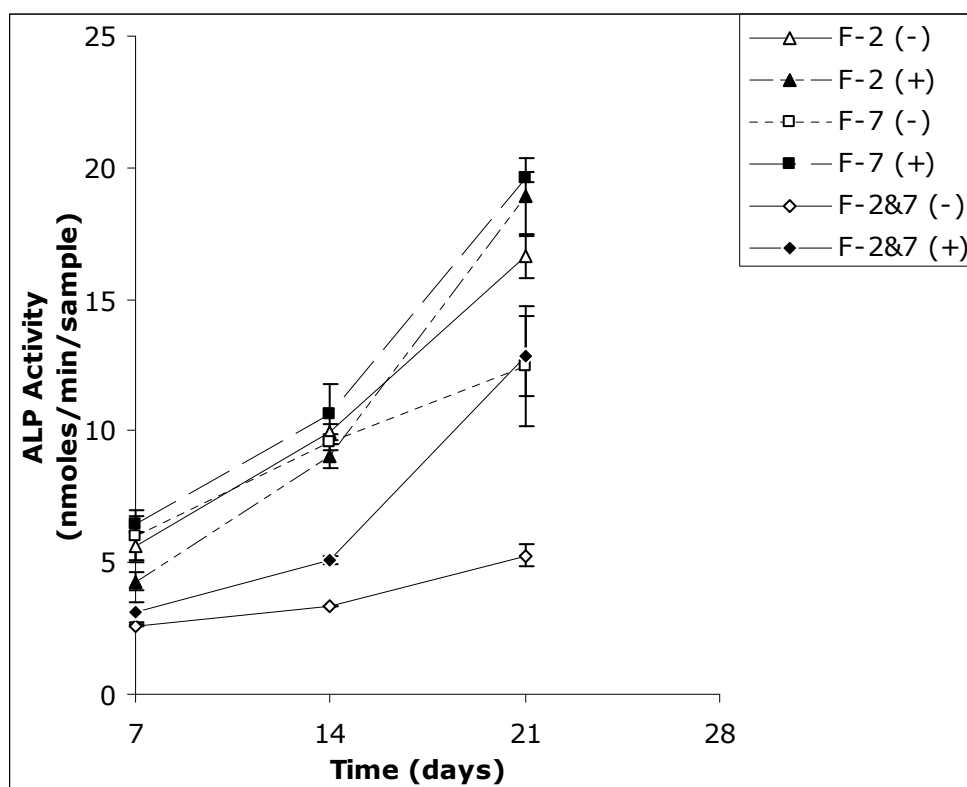


Figure 1. ALP activity in BMP (+) and BMP (-) foams.

ALP activity was detected to be significantly lower at all times in F-2&7 in comparison to F-2 and F-7 regardless of BMP presence, (the only exception was almost same levels of ALP activity in F-2&7 (+) and F-7 (-) on day 21) (*Fig. 12*). This data suggested that physical characteristics of foams (porosity, pore size distribution) had a significant effect on osteogenic differentiation [16]. Cell proliferation and ALP activity was detected to be inversely correlated in this study (*Fig. 11, Fig. 12*).

Again as osteogenic activity increases with down regulation of cell proliferation [152], lower ALP activities on F-2&7 (*Fig. 12*) fits in well with the enhanced cell proliferation (*Fig. 11*). However, on the 21st day of culture, ALP activity in F-2&7 (+) increased to a great extent and was almost the same with that of F-7(-) suggesting a considerable enhancement of ALP activity due to sequential delivery which overcame the effects of foam structure to a considerable degree.

ALP activity in F-7 (+) was observed to be significantly higher in comparison to F-7 (-) only on the 21st day of culture. However, higher ALP activity in F-2&7(+) in comparison to F-2&7 (-) was detected on both 14th and 21st days of culture. This data suggested that sequentially delivered BMP-2 and BMP-7 accelerated osteogenic differentiation in comparison to single delivery of either factor. The proliferation data showed that cell numbers on F-2&7 (+) and F-7 (+) foams are significantly lower than that of F-2&7 (-) on the 14th and F-7 (-) on the 21st day of culture, respectively (*Fig. 11*), which confirmed enhanced osteogenetic differentiation by ceased proliferation [152].

On the 7th day of culture, ALP activity in F-2 (-) was determined to be higher in comparison to F-2 (+) with a statistical significance (*Fig. 12*). However, at the end of culture, ALP activity in F-2 (+) caught up with F-2 (-) due to a higher rate of increase in ALP activity, especially after day 14. Therefore, enhancement of osteogenic differentiation can also be suggested to occur by single BMP-2 delivery from 4% microspheres although it is not as clear as in the single BMP-7 and sequential BMP-2 and BMP-7 delivery cases.

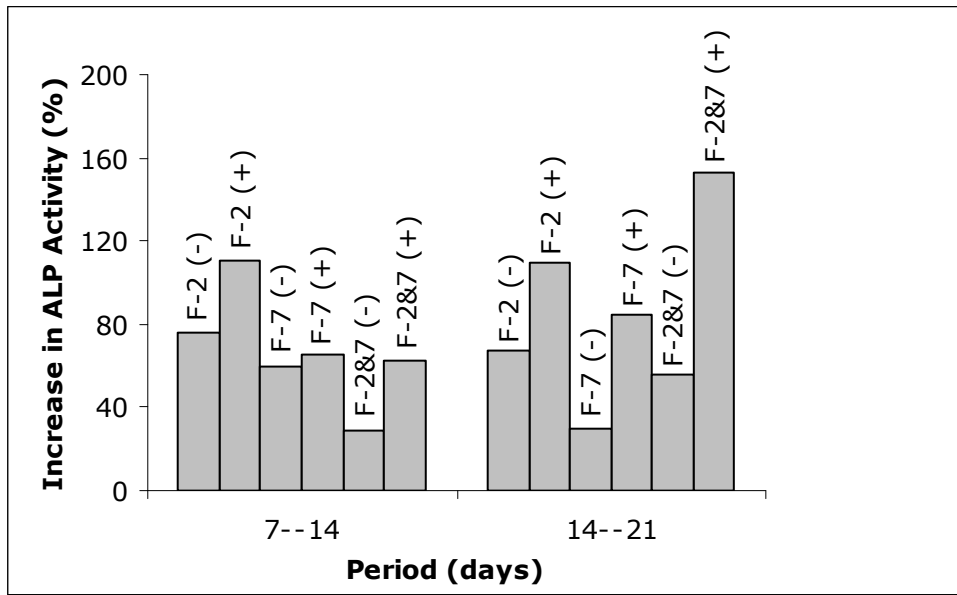


Figure 2. Percent ALP activity increase in BMP (+) and BMP (-) foams.

It was observed that increase in ALP activity at both periods (7 to 14 and 14 to 21) was always higher in BMP (+) samples in comparison to their corresponding BMP free controls (*Fig. 13*). The only exception was almost the same levels of increase between F-7 (-) and F-7 (+) between days 7 and 14. However, the difference became significant between days 14 and 21 in agreement with the slower release kinetics of BMP-7 delivering 10% microspheres (*Table 4*). The increase in ALP activity being higher in all positive samples in comparison to their negative controls at all times implied the effectiveness of BMP delivery from all three constructs even though the BMP encapsulation (*Table 7*), and therefore, release levels were low.

It can be seen that increase in osteogenic activity was higher between days 14 and 21 in comparison to increase between days 7 and 14 for both F-2&7 (+) and F-7 (+). The *in situ* release profiles, however, had revealed release of a large fraction of the contents in the first 7 days (*Fig. 2*). The observation of significant levels of effect of BMPs after day 14 suggested a slowing down of the BMP release from the foams in comparison to that from the free microspheres.

This is probably a result of diffusional restriction on growth factor mobility within the foam caused by the foam matrix.

The highest increase in ALP activity was observed in F-2 (+) and F-2&7 (+) between days 7-14 and days 14-21, respectively. This suggested a synergistic effect of the two sequentially delivered growth factors which dominated the effect of single delivery of either factor.

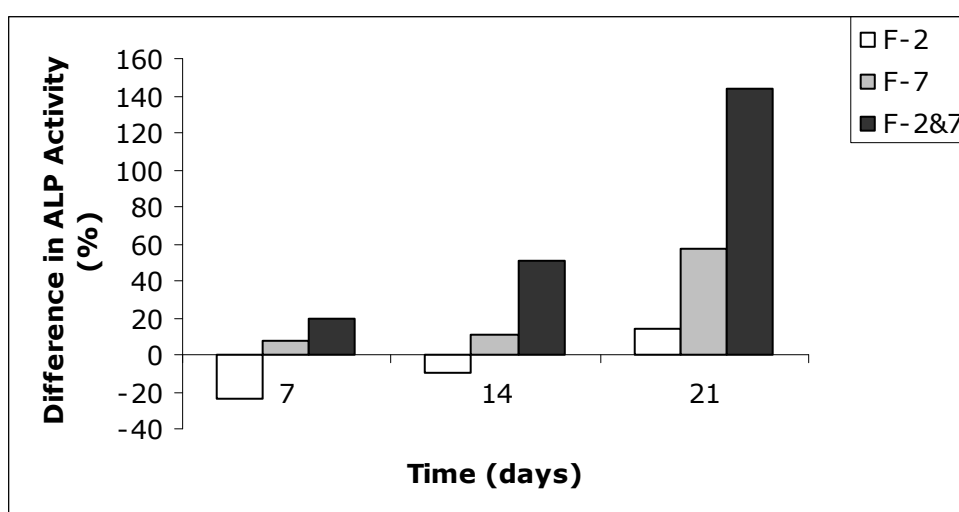


Figure 3. ALP activity difference between BMP (+) and BMP (-) foams.

The enhancement in ALP activity in BMP (+) samples in comparison to their corresponding negative controls was calculated in order to compare the 3 delivery systems (only BMP-2, only BMP-7, both BMP-2 and BMP-7) by eliminating the influence of foam characteristics on osteogenic activity (*Fig. 14*). An enhancement of osteogenic differentiation owing to BMP supply can be seen clearly for all groups at the end of 21 days of culture. ALP activities in F-2&7(+) were higher by 20% (day 7), 51% (day 14) and 144% (day 21), in comparison to F-2&7 (-) (*Fig. 14*). These numbers were only 7% (day 7), 11% (day 14) and 57% (day 21) for F-7 group and 14% (day 21) for F-2 group.

This data clearly demonstrates that combined delivery of BMP-2 and BMP-7 from different microsphere populations showed synergy and was much more effective in terms of osteogenic differentiation when compared to single BMP delivery from either of the microspheres. This was in accordance with other studies which reported better results with dual [115] and sequential [118] delivery of BMPs in comparison to single or simultaneous delivery, respectively.

3.6.3 Specific ALP Activity

Specific ALP activity was calculated by dividing total ALP activity to cell numbers to analyze ALP activity data without taking cell proliferation into account.

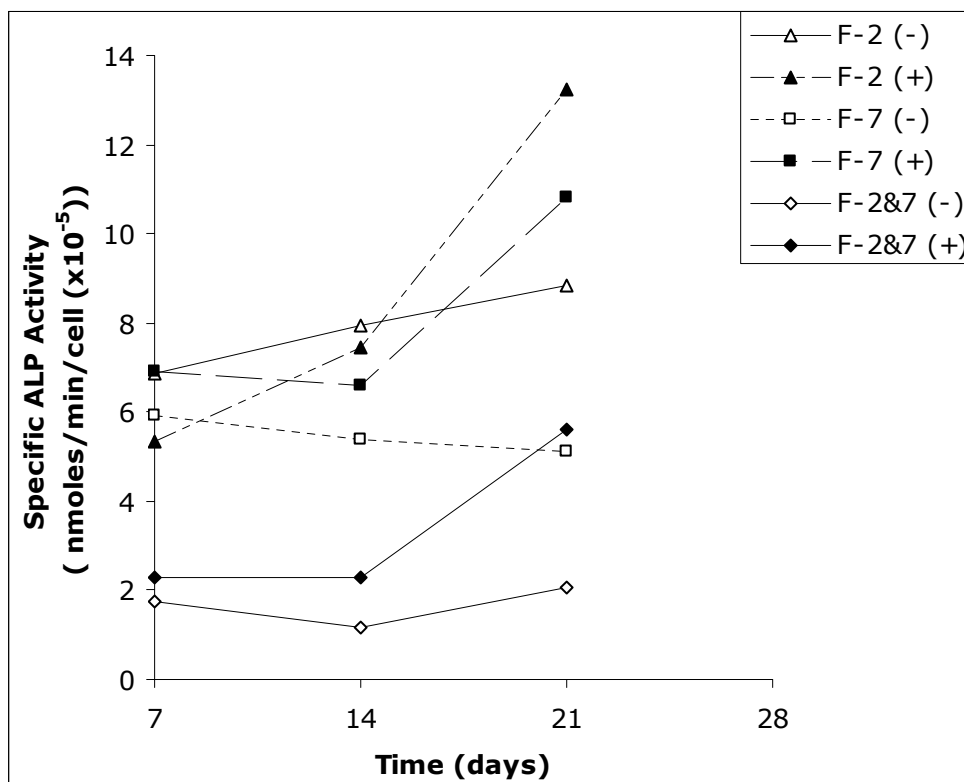


Figure 4. Specific ALP activity in BMP (+) and BMP (-) foams.

Specific ALP activity patterns (*Fig. 15*) were similar to that of total ALP activity patterns (*Fig. 12*) with lowest ALP activities in F-2&7 foams regardless of BMP presence at all times (the only exception was almost same levels of ALP activity in F-2&7 (+) and F-7 (-) on day 21). Moreover, there were large differences in specific ALP activities among BMP (-) samples. Highest specific ALP activity was detected in F-2 (-) at all times, followed by F-7 (-) and F-2&7 (-), respectively. These findings confirmed the direct effect of physical characteristics of foams on osteogenic differentiation regardless of their proliferative effects [16]. According to the results, F-2 was the most efficient foam type in terms of positive influence on osteogenic differentiation and was followed by F-7 and F-2&7, respectively (*Fig. 15*). This order was reverse for positive proliferative influence (*Fig. 11*). Still, it should be noted that specific ALP activity in F-2&7 (+) caught up with that of F-7 (-) on the 21st day of culture (*Fig. 15*) suggesting that sequential delivery of BMP-2 and BMP-7 overcame the effects of foam structure to a great degree after 14th day of culture.

Specific ALP activity in F-2&7 (-) did not differ between day 7 and 21 indicating ceased osteogenic differentiation in absence of BMP supply. In contrast, there was a significant increase in ALP activity in F-2&7 (+) foams from day 7 to 21 and specific ALP activities were higher at all times than that of F-2&7 (-) (*Fig. 15*). Similar observations were made for F-2 and F-7 categories. The only exception was F-2 (-), where a slight increase in specific ALP activity probably due to favorable foam characteristics was observed, still specific ALP activity in F-2 (+) was much higher than that of F-2 (-) at the end of culture. These observations confirmed effective performance of all BMP (+) systems in enhancing osteogenic differentiation.

It should be noted that although appreciable enhancement of osteogenic differentiation can be observed for all positive samples from day 7 to 21; the only appreciable enhancement among positive samples from day 7 to 14 was detected for BMP-2 (+) (*Fig. 15*). This is in agreement with the faster release rates of 4% microspheres (*Fig. 2*).

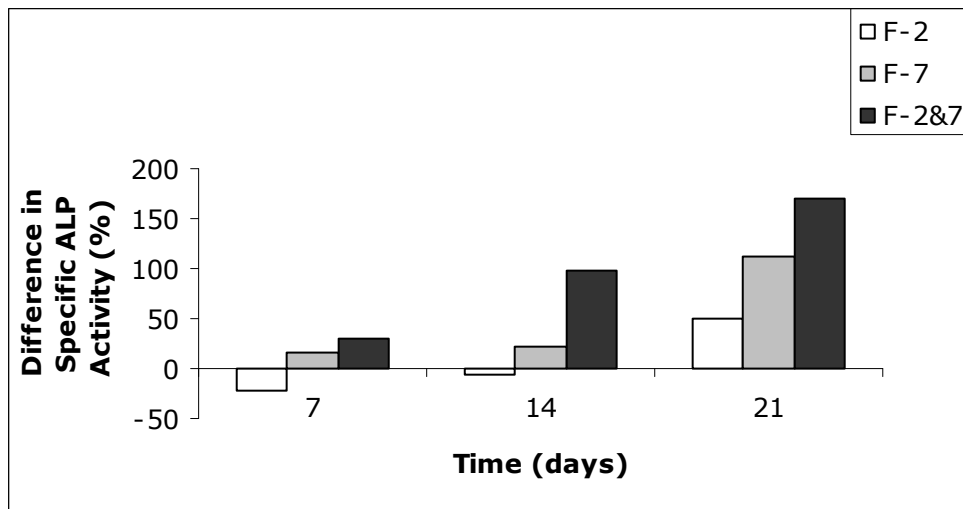


Figure 5. Specific ALP activity difference between BMP (+) and BMP (-) foams.

The enhancement in specific ALP activity in BMP (+) samples in comparison to their corresponding negative controls were calculated in order to compare the 3 delivery systems (only BMP-2, only BMP-7, both BMP-2 and BMP-7) by avoiding the influence of foam characteristics on osteogenic activity (*Fig. 16*). An enhancement of osteogenic differentiation owing to BMP supply can be seen clearly for all groups at the end of 21 days of culture. Specific ALP activities with F-2&7(+) were higher by 31% (day 7), 97% (day 14) and 170% (day 21), in comparison to F-2&7 (-) (*Fig. 16*). These numbers were 16% (day 7), 23% (day 14) and 112% (day 21) for F-7 group and 50% (day 21) for F-2 group. Again; this data clearly demonstrates that sequential and dual delivery of BMP-2 and BMP-7 from different microsphere populations was much more effective in terms of osteogenic differentiation when compared to single delivery performing systems.

3.6.4 Phalloidin Staining

Phalloidin staining of cells on foams was performed on the 21st day of culture and imaging was performed by Confocal Scanning Laser Microscope (CLSM).

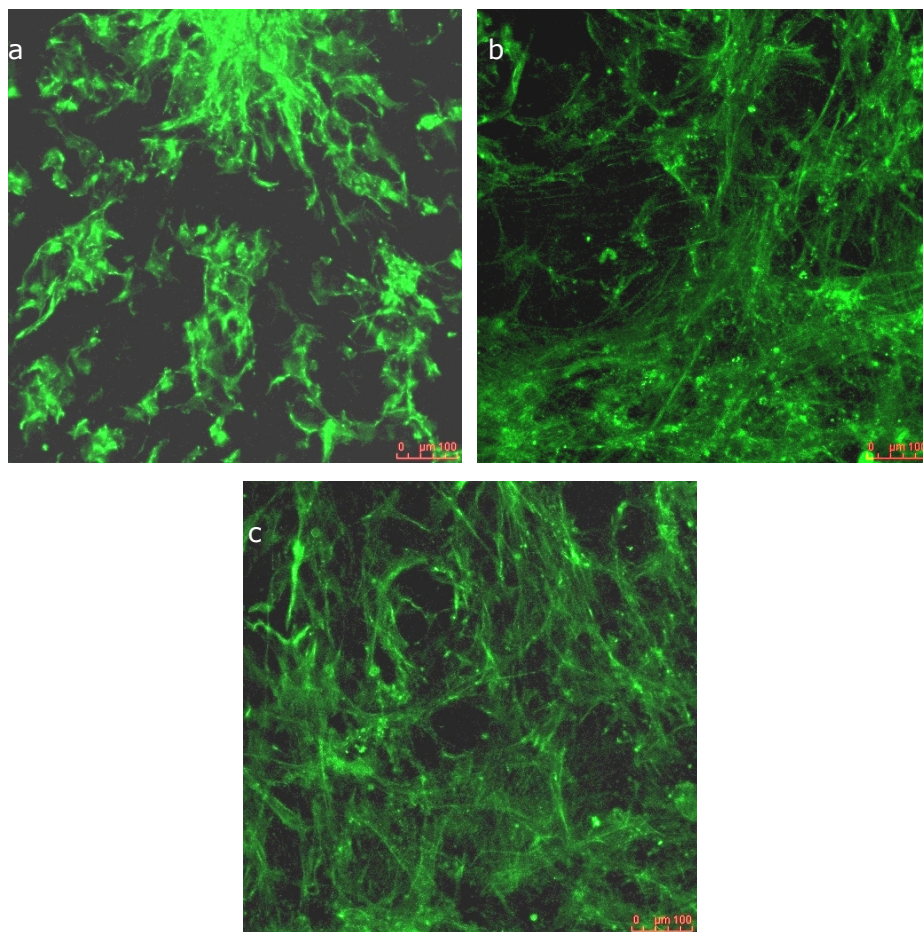


Figure 6. Phalloidin staining of cells observed with confocal laser scanning microscopy, (a) top view distribution and penetration of cells inside F-7 (-), (b) top view distribution and penetration of cells inside F-7 (+), (c) top view distribution and penetration of cells inside F-2&7 (+), (d) cross section of F-7 (-) (Z-axis direction), (e) cross section of F-7 (+) (Z-axis direction), (f) cross section of F-2&7 (+) (Z-axis direction). Magnification: x 20.

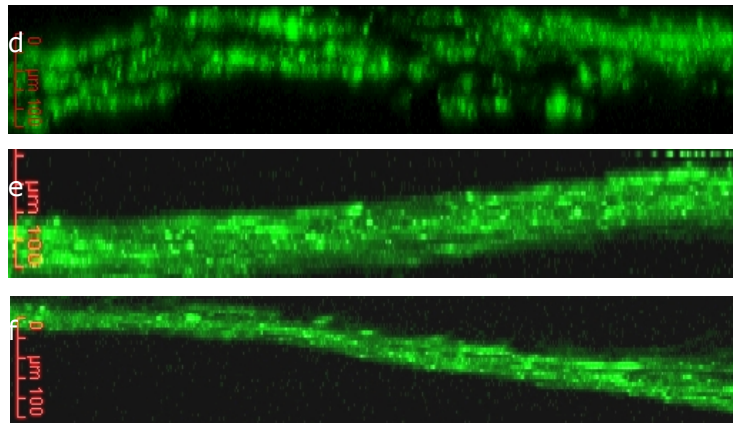


Figure 7. cont'd

CSLM images have revealed significant difference in cell morphologies and spreading between BMP loaded and unloaded foams (*Fig. 17*). Cells were in clumps on the BMP-free foams (*Fig. 17 a*) whereas well spread cells with osteoblast-like morphology and interconnecting extensions were observed on BMP loaded foams (*Fig. 17 b, c*). This was also confirmed with the cross section views where gaps between cells in unloaded foams can be seen (*Fig. 17 d*) in contrast to continuous layers of tightly connected cells in loaded foams (*Fig. 17 e, f*). It was observed that cell layer was tighter in F-2&7 in comparison to F-7 (*Fig. 17 e, f*). This could have led to closer contact between cells on F-2&7 enhancing proliferation and differentiation due to easier transmittance of intracellular signals.

3.6.5 Scanning Electron Microscopy

Scanning Electron Micrographs (SEM) of unseeded and seeded foams were taken after 21 days of culture. The foam is a microporous hydrophobic PLGA structure. The microspheres loaded into them, however, are complexes of polyelectrolytes and therefore at least partially hydrophilic.

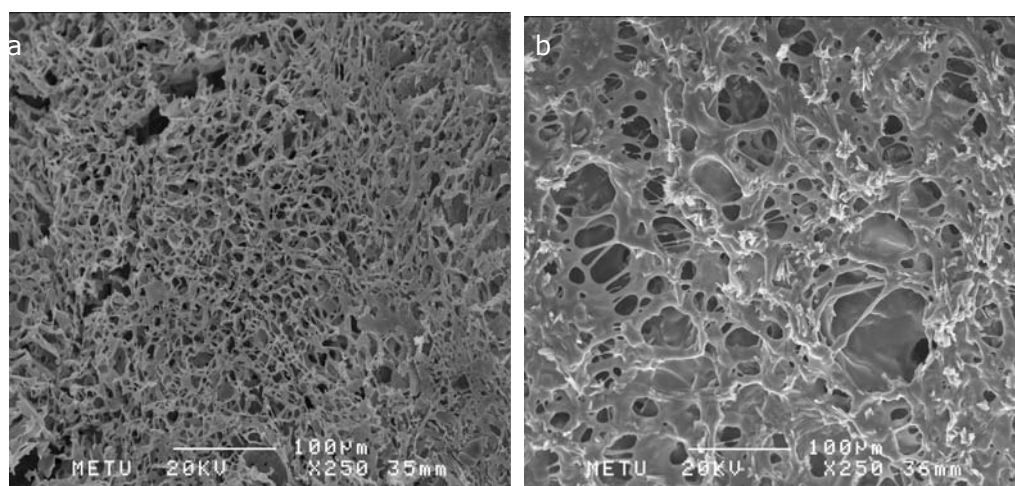


Figure 8. SEM images of cell seeded and unseeded F-7 (-) after 21 days of culture. (a) unseeded, (b) seeded. Magnification: x 250.

Figure 18 shows the cell seeding side (reverse of microsphere loaded side) of the foams. Comparison of unseeded F-7 (*Fig. 18 a*) and seeded F-7 (*Fig. 18 b*) clearly reveals that the foam is extensively populated with cells with their extensions spanning voids after 21 days of culture.

Figure 19 shows the microsphere loaded side of the foams and even the microspheres themselves. The spreading and interconnection of the extensions of cells on the PLGA foam structure is still observed as was on the other side (*Fig. 19 a*). The interconnected cells were observed to spread over microspheres entrapped in the foam indicating that cells also adhere to the slightly hydrophilic P₄VN-alginate complexes (*Fig. 19 b*).

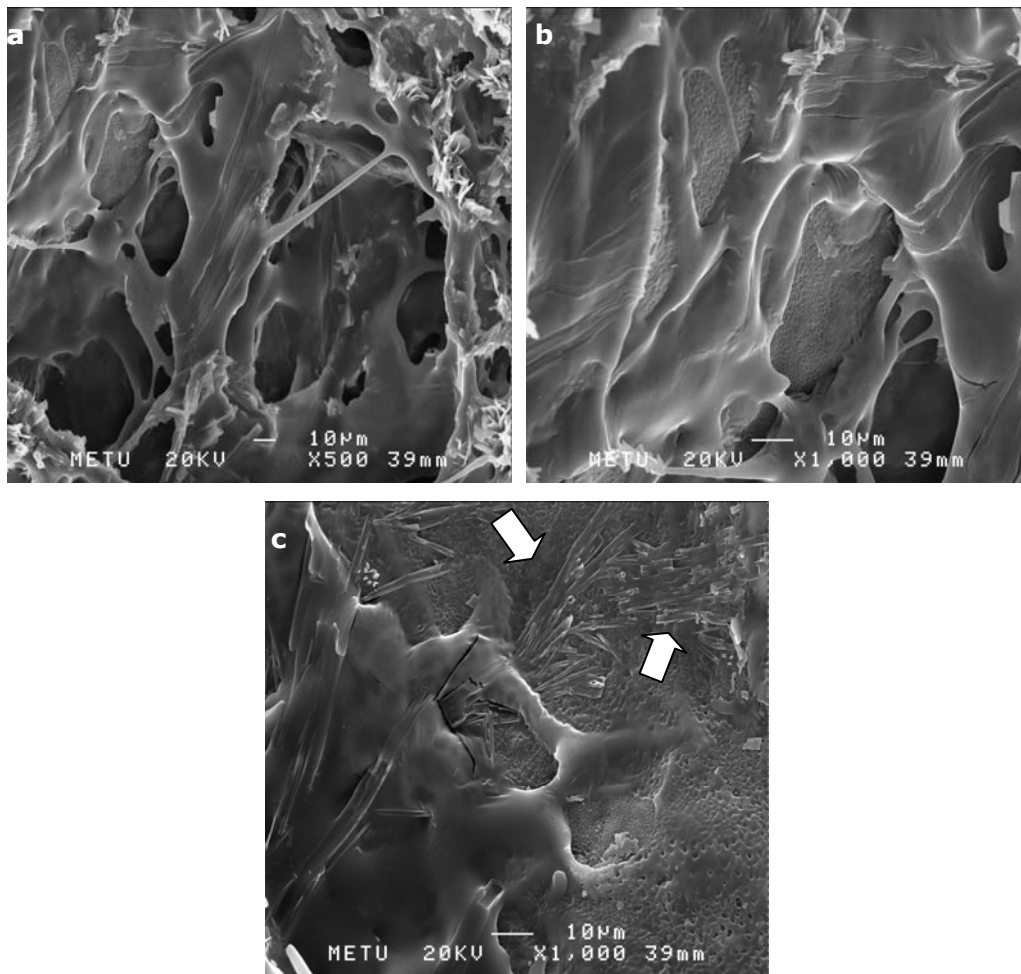


Figure 9. SEM images of cell seeded F-2&7 (+) after 21 days of culture. (a) x 500, (b) x 1000, (c) x 1000. Arrow heads indicate the crystal formation.

These SEMs also revealed the osteogenic activity of the cells. Mineral formation in the form of tubular crystals (observed but not chemically analyzed) that are indicative of osteogenic activity can be observed in Fig. 19 c (arrow heads).

CHAPTER 4

CONCLUSION

Microspheres were produced using polymer concentrations of 4%, 6%, 8% and 10%; and of these 4% microspheres were selected as 'early stage component' with the highest release rate and 10% microspheres were selected as 'long term release component' with the lowest release rate.

Decreasing crosslinking duration did not alter release rates, however, decreasing crosslinking temperature from RT to 4°C led to a significant increase in release rates of 4% and 10% microspheres which was unfavorable in terms of attaining sustained release. This increase was probably due to insufficient crosslinking at lower temperatures yielding less stable and compact structures. In the end, crosslinking temperature and duration were selected as RT and 1h, respectively, for use in other experiments.

Entrapment efficiencies were low in all groups under all preparation conditions. This was attributed to protein loss into the aqueous crosslinker solution during crosslinking. Reducing crosslinking period did not significantly increase entrapment efficiency whereas reducing crosslinking temperature from RT to 4°C led to a significant decrease in entrapment probably due to insufficient crosslinking at low temperatures.

SEM images of foams revealed a porous structure suitable for release and cell growth. Pore size distribution analysis demonstrated that microporosity was higher in F-4&10 in comparison to F-4 and F-7. Different physical characteristics of F-4&7 in comparison to F-4 and F-7 were also confirmed by stereomicroscopy.

Proliferation of cells on foams containing both populations of microspheres was higher at all time points regardless of BMP presence. It was concluded that depending on physical characteristics and independent of BMP presence, F-2&7 had highest positive influence on cell proliferation which was followed by F-7 and F-4, respectively. This conclusion was supported by stereomicroscope images and pore size distribution analysis which revealed microporosity necessary for proliferation decreased in the above order. Proliferation was lower in all BMP positive samples in comparison to their corresponding BMP free controls which suggested proliferation attenuation related enhancement of osteogenic activity with BMP supply.

Osteogenic differentiation was determined by Alkaline Phosphatase (ALP) Assay on 7th, 14th and 21st days of culture. ALP activity was detected in each group at all time points, regardless of BMP loading. Degree of osteogenic differentiation differed depending on foam characteristics, BMP presence and sequential BMP delivery. Total ALP activities were lowest at all time points for foams containing both microsphere populations; regardless of BMP presence. This was attributed to different physical characteristics of foams confirmed by the inverse correlation with proliferation. It was observed that increase in ALP activity during 21 days of culture was always higher in BMP (+) samples in comparison to their corresponding BMP free controls. On the other hand, specific ALP activities in all BMP-free foams did not significantly increase from day 7 to 21 whereas a significant increase in all BMP (+) foams was recorded. These findings revealed that BMP delivery from all three systems was effective in enhancing osteogenic differentiation.

To avoid the influence of foam characteristics on osteogenic activity, percent differences in total and specific ALP activities between BMP (+) samples and their corresponding negative controls were calculated. Results revealed that combined delivery of BMP-2 and BMP-7 from different microsphere populations showed synergy and was much more effective in terms of osteogenic differentiation when compared to single BMP delivery systems.

To sum up; BMP supply suppressed proliferation; however, foams which contained both microsphere populations had considerable positive influence on cell proliferation. Effects of single and combined delivery of growth factors were detected as enhanced osteogenic activity and the later strategy was more effective.

REFERENCES

1. Laurencin C. T., Ambrosio A. M. A., Borden M. D. and Cooper J. A., Jr., '*Tissue Engineering: Orthopedic Applications*', *Annu. Rev. Biomed. Eng.*, 01, 19-46 (1999).
2. Burg K. J. L., Porter S. and Kellam J. F., '*Biomaterial developments for bone tissue engineering*', *Biomaterials*, 22 (19), 2581-2593 (2001).
3. Hutmacher D.W., '*Scaffolds in tissue engineering bone and cartilage*', *Biomaterials*, 21 (24), 2529-2543 (2000).
4. Lee S-H. and Shin H., '*Matrices and scaffolds for delivery of bioactive molecules in bone and cartilage tissue engineering*', *Advan. Drug Del. Rev.*, 59 (4-5), 339-359 (2007).
5. Meyer U., Joos U. and Wiesmann H. P., '*Biological and biophysical principles in extracorporal bone tissue engineering: Part I*', *Intern. J. Oral and Maxillofacial Surg.*, 33 (4), 325-332 (2004).
6. Kokubo T., '*Apatite formation on surfaces of ceramics, metals and polymers in body environment*', *Acta Materialia* 46 (7), 2519-252 (1998).
7. Rose F. R. A. J. and Oreffo R. O. C., '*Bone Tissue Engineering: Hope vs Hype*', *Biochem. Biophys. Res. Communications*, 292 (1), 1-7 (2002).
8. Hutmacher D. W. and Garcia A. J., '*Scaffold-based bone engineering by using genetically modified cells*', *Gene*, 347 (1), 1-10 (2005).
9. Cancedda R., Dozin B., Giannoni P. and Quarto R. '*Tissue engineering and cell therapy of cartilage and bone*', *Matrix Biology*, 22 (1), 81-91 (2003).

10. So K., Fujibayashi S., Neo M., Anan Y., Ogawa T., Kokubo T. and Nakamura T., '*Accelerated degradation and improved bone-bonding ability of hydroxyapatite ceramics by the addition of glass*', *Biomaterials*, 27 (27), 4738-4744 (2006).
11. Li X., Feng Q. and Cui F., '*In vitro degradation of porous nano-hydroxyapatite/collagen/PLLA scaffold reinforced by chitin fibres*', *Mater. Sci. and Eng.: C*, 26 (4), 716-720 (2006).
12. Luo Z. S., Cui F. Z., Feng Q. L., Li H. D., Zhu X. D. and Spector M. '*In vitro and in vivo evaluation of degradability of hydroxyapatite coatings synthesized by ion beam-assisted deposition*', *Surface and Coatings Technol.*, 131 (1-3), 192-195 (2000).
13. Hasirci V., Lewandrowski K., Gresser J. D., Wise V. and Trantolo D. J., '*Versatility of biodegradable biopolymers: degradability and an in vivo application*', *J. Biotechnol.*, 86 (2), 135-150 (2001).
14. Jones J. and Hench L.L., '*Regeneration of trabecular bone using porous ceramics*', *Curr. Opin. Solid State Mater. Sci.*, 7, 301-307 (2003).
15. Gauthier O., Bouler J.M., Aguado E., Pilet P. and Daculsi G., '*Macroporous biphasic calcium phosphate ceramics: influence of macropore diameter and macroporosity percentage on bone ingrowth*', *Biomaterials*, 11 (3), 133-139 (1998).
16. Karageorgiou V. and Kaplan D., '*Porosity of 3D biomaterial scaffolds and osteogenesis*', *Biomaterials*, 26 (27), 5474-5491 (2005).
17. Mastrogiacomo M., Scaglione S., Martinetti R., Dolcini L., Beltrame F., Cancedda R. and Quarto R., '*Role of scaffold internal structure on in vivo bone formation in macroporous calcium phosphate bioceramics*', *Biomaterials*, 27, 3230-3237 (2006).

18. Cheung H-Y., Lau K-T., Lu T-P. and Hui D., '*A critical review on polymer-based bio-engineered materials for scaffold development*', *Composites Part B: Eng.*, 38 (3), 291-300 (2007).
19. Yang F., Williams C. G., Wang D., Lee H., Manson P. N. and Elisseeff J., '*The effect of incorporating RGD adhesive peptide in polyethylene glycol diacrylate hydrogel on osteogenesis of bone marrow stromal cells*', *Biomaterials*, 26 (30), 5991-5998 (2005).
20. de Taillac L. B., Porté-Durrieu M. C., Labrugère Ch., Bareille R., Amédée J. and Baquey Ch., '*Grafting of RGD peptides to cellulose to enhance human osteoprogenitor cells adhesion and proliferation*', *Composites Sci. Technol.*, 64 (6), 827-837 (2004).
21. Ma P. X., '*Scaffolds for tissue fabrication*', *Mater. Today*, 7 (5), 30-40 (2004).
22. Chung H. J., and Park T. G., '*Surface engineered and drug releasing pre-fabricated scaffolds for tissue engineering*', *Advan. Drug Delivery Rev.* 59 (4-5), 249-262 (2007).
23. Habraken W.J.E.M., Wolke J.G.C. and Jansen J.A., '*Ceramic composites as matrices and scaffolds for drug delivery in tissue engineering*', *Advan. Drug Del. Rev.* 59, 234-248 (2007).
24. Chen Z., Mo X. and Qing F., '*Electrospinning of collagen-chitosan complex*' *Mater. Letters*, 61 (16), 3490-3494 (2007).
25. Lee C. H., Singla A. and Lee Y., '*Biomedical applications of collagen*' *Intern. J. Pharms.*, 221 (1-2), 1-22 (2001).
26. Sanchez C., Arribart H. and Guille M.M., '*Biomimetism and bioinspiration as tools for the design of innovative materials and systems*', *Nat. Mater.*, 4, 277-288 (2005).

27. Seal B.R., Otero T. C. and Panitch A., '*Polymeric biomaterials for tissue and organ regeneration*', Mater. Sci. Eng., 34 (4-5), 147-230 (2001).
28. Martino A. D., Sittlinger M. and Risbud M. V., '*Chitosan: A versatile biopolymer for orthopaedic tissue-engineering*', Biomaterials, 26 (30), 5983-5990 (2005).
29. Eiselt P., Yeh J., Latvala R. K., Shea L. D. and Mooney D. J., '*Porous carriers for biomedical applications based on alginate hydrogels*', Biomaterials, 21, 1921-1927 (2000).
30. Veparia C. and Kaplan D. L., '*Silk as a biomaterial*', Prog. Poly. Sci. 32 (8-9), 991-1007 (2007).
31. Wang Y., Kim H-J., G. V-Novakovic and D. L. Kaplan, '*Stem cell-based tissue engineering with silk biomaterials*', Biomaterials, 27 (36), 6064-6082 (2006).
32. Kim J., Kim I. S., Cho T. H., Lee K. B., Hwang S. J., Tae G., Noh I., Lee S. H., Park Y. and Sun K., '*Bone regeneration using hyaluronic acid-based hydrogel with bone morphogenic protein-2 and human mesenchymal stem cells*', Biomaterials, 28 (10), 1830-1837 (2007).
33. Grigolo B., Roseti L., Fiorini M., Fini M., Giavaresi G., Aldini N. N., Giardino R. and Facchini A., '*Transplantation of chondrocytes seeded on a hyaluronan derivative (hyaff-11) into cartilage defects in rabbits*', Biomaterials 22 (17), 2417-2424 (2001).
34. Chen G. Q. and Wu Q., '*The application of polyhydroxyalkanoates as tissue engineering materials*', Biomaterials, 26, 6565-78 (2005).
35. Doyle C., Tanner E. T. and Bonfield W., '*In vitro and in vivo evaluation of polyhydroxybutyrate and of polyhydroxybutyrate reinforced with hydroxyapatite*', Biomaterials, 12, 841-847 (1991).

36. Köse G. T., Kenar H., Hasırcı N. and Hasırcı V., '*Macroporous poly(3-hydroxybutyrate-co-3-hydroxyvalerate) matrices for bone tissue engineering*', *Biomaterials*, 24 (11), 1949-1958 (2003).
37. Köse G. T., Korkusuz F., Korkusuz P., Puralı N., Özkul A. and Hasırcı V., '*Bone generation on PHBV matrices: an in vitro study*', *Biomaterials*, 24 (27), 4999-5007 (2003).
38. Rezwan K., Chen Q.Z., Blaker J.J. and Boccaccini A. R., '*Biodegradable and bioactive porous polymer/inorganic composite scaffolds for bone tissue engineering*', *Biomaterials* 27, 3413-3431 (2006).
39. Andrew S. D., Phil G. C. and Marra K. G., '*The influence of polymer blend composition on the degradation of polymer/hydroxyapatite biomaterials*' *J. Mater. Sci: Mater. Med.*, 12, 673-677 (2001).
40. Heidemann W., Jeschkeit S., Ruffieux K., Fischer J. H., Wagner M. and Kruger G., Wintermantel E. and Gerlach K. G., '*Degradation of poly(D,L)lactide implants with or without addition of calciumphosphates in vivo*', *Biomaterials*, 22, 2371-81 (2001).
41. Li H. Y., Chang J. '*pH-compensation effect of bioactive inorganic fillers on the degradation of PLGA*', *Compos. Sci. Technol.*, 65, 2226-2232 (2005).
42. Pang L., Hu Y., Yan Y., Liu L., Xiong Z., Wei Y. and Bai J., '*Surface modification of PLGA/ β -TCP scaffold for bone tissue engineering: Hybridization with collagen and apatite*', *Surface and Coatings Technol.*, Available online 2007
43. Kim S-S., Park M. S., Jeon O., Choi C. Y., Kim B-S., '*Poly(lactide-co-glycolide)/hydroxyapatite composite scaffolds for bone tissue engineering*' *Biomaterials*, 27 (8), 1399-1409 (2006).

44. Kim H., Suh H., Jo S. A., Kim H. W., Lee J. M., Kim E. H., Reinwald Y., Park S-H., Min B-H. and Jo I., '*In vivo bone formation by human marrow stromal cells in biodegradable scaffolds that release dexamethasone and ascorbate-2-phosphate*', Biochem. Biophys. Res. Communications, 332 (4), 1053-1060 (2005).
45. Wu L. and Ding J., '*Effects of porosity and pore size on in vitro degradation of three-dimensional porous poly(D,L-lactide-co-glycolide) scaffolds for tissue engineering*', J. Biomed. Mater. Res., 75A (4), 767-777 (2005).
46. Rich J., Jaakkola T., Tirri T., Narhi T., Y-Urpo A. and Seppala J., '*In Vitro evaluation of poly(ϵ -caprolactone-co-DL-lactide)/bioactive glass composites*', Biomaterials, 23 (10), 43-2150 (2002).
47. Yang S., Leong K. F., Du Z. and Chua C. K., '*The design of scaffolds for use in tissue engineering. Part I. Traditional factors*', Tissue Eng., 7, 679-689 (2001).
48. Yaszewski M. J., Payne R. G., Hayes W. C., Langer R., Aufdemorte T. B. and Mikos A. G., '*The ingrowth of new bone tissue and initial mechanical properties of a degrading polymeric composite scaffold*', Tissue Eng., 1, 41-52 (1995).
49. Hench L. L., Splinter R.J. and Allen W. C., '*Bonding mechanisms at the interface of ceramic prosthetic materials*', J. Biomed. Mater. Res Symp. 2, 117-141 (1971).
50. Li H. Y., Du R. L. and Chang J., '*Fabrication, characterization, and in vitro degradation of composite scaffolds based on PHBV and bioactive glass*', J. Biomater. Appl., 20, 137-55 (2005).

51. Liang H., Wan Y.Z., He F., Huang Y., Xu J. D., Li J. M., Wang Y.L. and Zhao Z. G., '*Bioactivity of Mg-ion-implanted zirconia and titanium*', App. Surface Sci., 253 (6), 3326-3333 (2007).
52. Lu H. H., Tang A., Oh S. C., Spalazzi J. P. and Dionisio K., '*Compositional effects on the formation of a calcium phosphate layer and the response of osteoblast-like cells on polymer-bioactive glass composite*'. Biomaterials, 26, 6323-6334 (2005).
53. Gatti A. M., Valdre G., and Andersson O. H., '*Analysis of the in vivo reactions of a bioactive glass in soft and hard tissue*', Biomaterials, 15, 208-12 (1994).
54. Roether J. A., Gough J.E. , Boccaccini A. R., Hench L. L., Maquet V. and Jerome R., '*Novel bioresorbable and bioactive composites based on bioactive glass and polylactide foams for bone tissue engineering*', J. Mater. Sci: Mater. Med., 13, 1207-1214 (2002).
55. Itskovitz-Eldor J., Schuldiner M., Karsenti D., Eden A., Yanuka O., Amit M., Soreq H. and Benvenisty N., '*Differentiation of human embryonic stem cells into embryoid bodies compromising the three embryonic germ layers*', Mol. Med., 6, 88-95 (2000).
56. Olivier V., Faucheux N. and P. Hardouin, '*Biomaterial challenges and approaches to stem cell use in bone reconstructive surgery*' DDT, 9 (18), 803-811 (2004).
57. E. M. Horwitz, '*Stem cell plasticity: the growing potential of cellular therapy*', Archives of Med. Res., 34 (6), 600-606 (2003).
58. Croft A.P. and Przyborski S.A., '*Mesenchymal stem cells from the bone marrow stroma: basic biology and potential for cell therapy*', Curr. Anaesthesia & Critical Care, 15, 410-417 (2004).

59. Bruder S. P. and Caplan A. I., '*Bone regeneration through cellular engineering*' Principles of Tissue Eng. 683-696 (2000).
60. Fehrer C. and Lepperdinger G., '*Mesenchymal stem cell aging*', Experimental Gerontology, 40, 926-930 (2005).
61. Deliloglu-Gurhan S.I., Vatansever H.S., Ozdal-Kurt F. and Tuglu I., '*Characterization of osteoblasts derived from bone marrow stromal cells in a modified cell culture system*', Acta Histochemica, 108 (1), 49-57 (2006).
62. Pittenger M. F., Mackay A. M., Beck S. C., Jaiswal R. K., Douglas R. , Mosca J. D., Moorman M. A., Simonetti D. W., Craig S., and Marshak D. R., '*Multilineage potential of adult human mesenchymal stem cells*', Science, 284 (5411), 143-147 (1999).
63. Digirolamo C. M., Stokes D., Colter D., Phinney D. G., Class R. and Prockop D. J., '*Propagation and senescence of human marrow stromal cells in culture: a simple colony-forming assay identifies samples with the greatest potential to propagate and differentiate*', Br. J. Haematol., 107 (2), 275-81 (1999).
64. Bianco P., Riminucci M., Gronthos S. and Robey P.G., '*Bone marrow stromal stem cells: Nature, biology, and potential applications*', Stem Cells, 19, 180-192 (2001).
65. Oreffo R.O. and Triffit J.T., '*In vitro and in vivo methods to determine the interactions of osteogenic cells with biomaterials*', J. Mater. Sci. Mater. Med., 10, 607-611 (1999).
66. Ohgushi H. and Caplan A. I., '*Stem cell technology and bioceramics: from cell to gene engineering*', J. Biomed. Mater. Res., 48, 913-927 (1999).

67. Flautre B., Anselme K., Delecourt C., Lu C., Hardouin P. and Descamps M., '*Histological aspects in bone regeneration of an association with porous hydroxyapatite and bone marrow cells*', J. Mater. Sci. Mater. Med., 10, 811–814 (1999).
68. Cancedda R., Bianchi G., Derbeis, A. and Quarto R., '*Cell therapy for bone disease: A review of current status*', Stem Cells, 21, 610-619 (2003).
69. Koc O. N., Day J., Nieder M., Gerson S. L., Lazarus H. M. and Krivit W., '*Allogeneic mesenchymal stem cell infusion for treatment of metachromatic leukodystrophy (MLD) and Hurler syndrome (MPS-IH)*', Bone Marrow Transplant, 30 (4), 215–222 (2002).
70. Fouillard L., Bensidhoum M., Bories D., Bonte H., Lopez M., Moseley A. M., Smith A., Lesage S., Beaujean F., Thierry D., Gourmelon P., Najman A. and Gorin N. C., '*Engraftment of allogeneic mesenchymal stem cells in the bone marrow of a patient with severe idiopathic aplastic anemia improves stroma*', Leukemia, 17 (2), 474–476 (2003).
71. Horwitz E. M., Prockop D. J., Fitzpatrick L. A. Koo W. W. K., Gordon P. L., Neel M., Sussman M., Orchard P., Marx J. C., Pyeritz R. E. and Brenner M. K., '*Transplantability and therapeutic effects of bone marrow-derived mesenchymal cells in children with osteogenesis imperfecta*', Nature Med., 5, 309-313 (1999).
72. Aggarwal S. and Pittenger M. F., '*Human mesenchymal stem cells modulate allogeneic immune cell responses*', Blood, 105, 1815–1822 (2005).
73. Griffith L. G. and Naughton G., '*Tissue Engineering-Current Challenges and Expanding Opportunities*', Science, 295 (5557), 1009-1014 (2002).
74. Connolly J. F., '*Clinical use of marrow osteoprogenitor cells to stimulate osteogenesis*' Clin. Orthop. 355, S257–S266 (1998).

75. Horwitz E. M., Prockop D. J., Gordon P.L., Koo W.W., Fitzpatrick L.A., Neel M.D., McCarville M. E., Orchard P. J., Pyeritz R. E., and Brenner M. K., '*Clinical responses to bone marrow transplantation in children with severe osteogenesis imperfecta*', *Blood*, 5, 1227–1231 (2001).
76. Mauney J.R., Kaplan D. L. and Volloch V., '*Matrix-mediated retention of osteogenic differentiation potential by human adult bone marrow stromal cells during ex vivo expansion*', *Biomaterials*, 25, 3233–3243 (2004).
- 77 Kon E., Muraglia A., Corsi A., Bianco P., Marcacci M., Martin I., Boyde A., Ruspantini I., Chistolini P., Rocca M., Giardino R., Cancedda R. and Quarto R. '*Autologous bone marrow stromal cells loaded onto porous hydroxyapatite ceramic accelerate bone repair in critical-size defects of sheep long bones*', *J. Biomed. Mater. Res.* 49 (3), 328-337 (2000).
78. Quarto R., Mastrogiacomo M., Cancedda R., Kutepov S. M., Mukhachev V., Lavroukov A., Kon E., and Marcacci M., '*Repair of large bone defects with the use of autologous bone marrow stromal cells*', *N. Engl. J. Med.*, 344 (5), 385–6 (2001).
79. Marcacci M., Kon K., Moukhachev V., Lavroukov A., Kutepov S., Quarto R., Mastrogiacomo M., and Cancedda R., '*Stem cells associated with macroporous bioceramics for long bone repair: 6 to 7 year outcome of a pilot clinical study*', *Tissue Eng.*, 13, 947–955 (2007).
80. Street J., Bao M., deGuzman L., Bunting S., Peale Jr F.V., Ferrara N., Steinmetz H., Hoeffel J., Cleland J.L., Daugherty A., van Bruggen N., Redmond H. P., Carano R. A. and Filvaroff E. H., '*Vascular endothelial growth factor stimulates bone repair by promoting angiogenesis and bone turnover*', *Proc. Natl. Acad. Sci.*, 99, 9656–9661 (2002).
81. Schliephake H., '*Bone growth factors in maxillofacial skeletal reconstruction*', *Int. J.Oral Maxillofac. Surg.*, 31, 469–484 (2002).

82. Bianda T., Hussain M. A., Glatz Y, Bouillon R., Froesch E. R. and Schmid C., '*Effects of short-term insulin-like growth factor-I or growth hormone treatment on bone turnover, renal phosphate reabsorption and 1,25 dihydroxyvitamin D3 production in healthy man*', J. Intern. Med., 241, 143–150 (1997).
83. Chen F. M., Zhao Y. M., Wu H., Deng Z. H., Wang Q. T., Zhou W., Liu Q., Dong G. Y., Li K., Wu Z. F. and Jin Y., '*Enhancement of periodontal tissue regeneration by locally controlled delivery of insulin-like growth factor-I from dextran-co-gelatin microspheres*', J. Control. Release, 114, 209–222 (2006).
84. Nakamura K., Kawaguchi H., Aoyama I., Hanada K., Hiyama Y., Awa T., Tamura M., and Kurokawa T., '*Stimulation of bone formation by intraosseous application of recombinant basic fibroblast growth factor in normal and ovariectomized rabbits*', J. Orthop. Res. 15, 307–313 (1997).
85. Quarto N. and Longaker M.T., '*FGF-2 inhibits osteogenesis in mouse adipose tissue-derived stromal cells and sustains their proliferative and osteogenic potential state*', Tissue Eng., 12, 1405–1418 (2006).
86. Varkey M., Kucharski C., Haque T., Sebald W. and Uludag H., '*In vitro osteogenic response of rat bone marrow cells to bFGF and BMP-2 treatments*', Clin. Orthop. Relat. Res., 443, 113–123 (2006).
87. Kawaguchi H., Kurokawa T., Hanada K., Hiyama Y., Tamura M., Ogata E. and Matsumoto T., '*Stimulation of fracture repair by recombinant human basic fibroblast growth factor in normal and streptozotocin diabetic rats*', Endocrinology, 135, 774–781 (1994).
88. Kato T., Kawaguchi H., Hanada K., Aoyama I., Hiyama Y., Nakamura T., Kuzutani K. Tamura M., Kurokawa T. and Nakamura K., '*Single local injection of recombinant fibroblast growth factor-2 stimulates healing of segmental bone defects in rabbits*', J. Orthop. Res., 16, 654–659 (1998).

89. Murphy W. L., Peters M. C., Kohn D. H. and Mooney D. J., '*Sustained release of vascular endothelial growth factor from mineralized poly(lactide-co-glycolide) scaffolds for tissue engineering*', *Biomaterials*, 21 (24), 2521-2527 (2000).
90. Mikos A. G., Sarakinos G., Ingber D. E., Vacanti J. and Langer R., '*Prevascularization of porous biodegradable polymers*', *Biotech. Bioeng.*, 42, 716-723 (1993).
91. Mooney D. J., Kaufmann P. M., Sano K., McNamara K. M., Vacanti J. P. and Langer R., '*Transplantation of hepatocytes using porous, biodegradable sponges*', *Transplant Proc.*, 26, 3425-3426 (1994).
92. Hsiong S. X. and Mooney D. J., '*Regeneration of vascularized bone*', *Periodontol.* 2000, 41, 109-122 (2006).
93. Wozney J. M., Rosen V., Celeste A. J., Mitsock L. M., Whitters M.J., Kriz R. W., Hewick R. M. and Wang E. A., '*Novel regulators of bone formation: molecular clones and activities*', *Science*, 242, 1528-1534 (1988).
94. Celeste A. J., Iannazzi J. A., Taylor R. C., Hewick R. M., Rosen V., Wang E.A. and Wozney J.M., '*Identification of transforming growth factor beta family members present in bone-inductive protein purified from bovine bone*', *Proc. Natl. Acad. Sci.*, 87, 9843-9847 (1990).
95. Erlebacher A., Filvaroff E.H., Ye J.Q. and Derynck R., '*Osteoblastic responses to TGF-beta during bone remodeling*', *Mol. Biol. Cell*, 9, 1903-1918 (1998).
96. Pucéat M., '*TGFβ in the differentiation of embryonic stem cells*', *Cardiovascular Res.*, 74 (2), 256-261 (2007).

97. Ehrhart N.P., Hong L., Morgan A.L., Eurell J.A. and Jamison R.D., '*Effect of transforming growth factor-beta1 on bone regeneration in critical-sized bone defects after irradiation of host tissues*', Am. J. Vet. Res., 66, 1039–1045 (2005).
98. Ramoshebi L.N., Matsaba T.N., Teare J., Renton L., Patton J., and Ripamonti U., '*Tissue engineering: TGF-beta superfamily members and delivery systems in bone regeneration*', Expert Rev. Mol. Med., 1–11 (2002).
99. Broderick E., Infanger S., Turner T.M. and Sumner D.R., '*Depressed bone mineralization following high dose TGF-beta1 application in an orthopedic implant model*', Calcif. Tissue Int., 76, 379–384 (2005).
100. Kirker-Head C. A., '*Potential applications and delivery strategies for bone morphogenetic proteins*', Advan. Drug Delivery Rev., 43 (1), 65-69 (2000).
101. Urist M.R., '*Bone formation by autoinduction*', Science, 150, 893–899 (1965).
102. Urist M. R., Strates B. S., '*Bone morphogenetic protein*', J. Dent. Res., 50, 1392-1406 (1971).
103. Cheung A. and Phillips A. M., '*Bone morphogenetic proteins in orthopaedic surgery*', Curr. Orthop. 20 (6), 424-429 (2006).
104. Vaibhav B., Nilesh P., Vikram S. and Anshul C., '*Bone morphogenic protein and its application in trauma cases: A current concept update*', Injury, Available online 2007.
105. Yasko A. W., Lane J. M., Fellingner E. J., Rosen V., Wozney J. M. and Wang E. A., '*The healing of segmental bone defects, induced by recombinant human bone morphogenetic protein (rhBMP-2). A radiographic, histological and biomechanical study in rats*', J. Bone Joint Surg. Am., 74, 659-670 (1992).

106. Bostrom M., Lane J. M., Tomin E., Browne M., Berberian W., Turek T., Smith J., Wozney J., and Schildhauer T., '*Use of bone morphogenetic protein-2 in the rabbit ulnar nonunion model*', Clin. Orthop., 327, 272-82 (1996).
107. Cook S. D., Baffes G. C., Wolfe M. W., Sampath T. K., Rueger D. C. and Whitecloud T. S., '*The effect of recombinant human osteogenic protein-1 on healing of large segmental bone defects*', J. Bone Joint Surg. Am., 76, 827-38 (1994).
108. Gerhart T. N., Kirker-Head C. A. and Kriz M. J., '*Healing segmental femoral defects in sheep using recombinant human bone morphogenic protein*', Clin. Orthop., 293, 317-326 (1993).
109. Bobis S., Jarocha D., and Majka M., '*Mesenchymal stem cells: characteristics and clinical applications*', Folia Histochemica et Cytobiologica, 44 (4), 215-230 (2006).
110. Shea C. M., Edgar C. M., Einhorn T. A., and Gerstenfeld L. C., '*BMP treatment of C3H10T1/2 mesenchymal stem cells induces both chondrogenesis and osteogenesis*', J. Cell Biochem., 90 (6), 1112-27 (2003).
111. Cowan C. M., Soo C., Ting K. and B. Wu, '*Evolving Concepts in Bone Tissue Engineering*', Curr. Topics in Developmental Biology, 66, 239-285 (2005)
112. Luginbuehl V., Meinel L., Merkle H. P. and Gander B., '*Localized delivery of growth factors for bone repair*', Europ. J. Pharma. Biopharma., 58 (2), 197-208 (2004).
113. P. B. , Silva G. A. , Baran E. T. and Reis R. L., '*Drug delivery therapies I: General trends and its importance on bone tissue engineering applications*', Malafaya Curr. Opin. Solid State Mater. Sci., 6, 283-295 (2002).

114. Luu H. H., Song W-X., Luo X., Manning D., Luo J., Deng Z., Sharff K., Montag A. G., Haydon R. C. and He T-C., '*Distinct Roles of Bone Morphogenetic Proteins in Osteogenic Differentiation of Mesenchymal Stem Cells*', J. Orthop. Res., 25 (5), 665-677 (2007).
115. Simmons C. A., Alsberg E., Hsiong S., Kim W. J. and Mooney D. J., '*Dual growth factor delivery and controlled scaffold degradation enhance in vivo bone formation by transplanted bone marrow stromal cells*', Bone, 35 (2), 562-569 (2004).
116. Vonau R. L., Bostrom M. P., Aspenberg P. and Sams A.E., '*Combination of growth factors inhibits bone ingrowth in the bone harvest chamber*', Clin. Orthop., 243-251 (2001).
117. Schmidmaier G., Wildemann B., Gabelein T., Heeger J., Kandziora F., Haas N. P. and Raschke M., '*Synergistic effect of IGF-I and TGF-beta1 on fracture healing in rats: single versus combined application of IGF-I and TGF-beta1*', Acta Orthop. Scand., 74, 604-610 (2003).
118. Raiche A. T. and Puleo D. A., '*In vitro effects of combined and sequential delivery of two bone growth factors*', Biomaterials, 25, 677-685 (2004).
119. Whang K., Goldstick T. K., Healy K. E. '*A biodegradable polymer scaffold for delivery of osteotropic factors*', Biomaterials, 21, 2545-2551 (2000).
120. Ueda H., Hong L., Yamamoto M., Shigeno K., Inoue M., Toba T., Yoshitani M., Nakamura T., Tabata Y. and Shimizu Y., '*Use of collagen sponge incorporating transforming growth factor-beta1 to promote bone repair in skull defects in rabbits*', Biomaterials, 23, 1003-1010 (2002).
121. Ribeiro A. J., Silva C., Ferreira D. and Veiga F., '*Chitosan-reinforced alginate microspheres obtained through the emulsification/internal gelation technique*', Europ. J. Pharma. Sci., 25 (1), 31-40 (2005).

122. Wang X., Wenk E., Hu X., Castro G. R., Meinel L., Wang X., Li C., Merkle H., Kaplan D. L., '*Silk coatings on PLGA and alginate microspheres for protein delivery*', *Biomaterials*, 28 28 (2007) 4161-4169.
123. Sokolsky-Papkov M., Agashi K., Olaye A., Shakesheff K. and Domb A. J., '*Polymer carriers for drug delivery in tissue engineering*', *Advan. Drug Delivery Rev.*, 59, 187–206 (2007).
124. Freiberg S. and Zhu X. X., '*Polymer microspheres for controlled drug release*', *Intern. J. Pharma.*, 282 (1-2), 1-18 (2004).
125. Baldwin S. P. and Saltzman W. M., '*Materials for protein delivery in tissue engineering*', *Advan. Drug Delivery Rev.*, 33, 71–86 (1998).
126. Kakish H. F., Tashtoush B., Ibrahim H. G. and Najib N. M., '*A novel approach for the preparation of highly loaded polymeric controlled release dosage forms of diltiazem HCl and diclofenac sodium*', *Eur. J. Pharma. Biopharma.*, 54, 75–81 (2002).
127. Yang Y-Y., Chung T-S., Bai X-L. and Chan W-K., '*Effect of preparation conditions on morphology and release profiles of biodegradable polymeric microspheres containing protein fabricated by double-emulsion method*', *Chem. Eng. Sci.*, 55, 2223–2236 (2000).
128. Kim S. E., Park J. H., Cho Y. W., Chung H., Jeong S. Y., Lee E. B. and Kwon I. C., '*Porous chitosan scaffold containing microspheres loaded with transforming growth factor- β 1: Implications for cartilage tissue engineering*', *J. Control. Release*, 91 (3), 365-374 (2003).
129. Wei G., Jin Q., Giannobile W. V. and Ma P. X., '*The enhancement of osteogenesis by nano-fibrous scaffolds incorporating rhBMP-7 nanospheres*', *Biomaterials*, 28, 2087-2096 (2007).

130. DeFail A. J., Chu C. R., Izzo N. and Marra K. G., '*Controlled release of bioactive TGF- β 1 from microspheres embedded within biodegradable hydrogels*', *Biomaterials*, 27 (8), 1579-1585 (2006).
131. Hosseinkhani H., Hosseinkhani M., Khademhosseini A. and Kobayashi H., '*Bone regeneration through controlled release of bone morphogenetic protein-2 from 3D tissue engineered nano-scaffold*', *J. Control. Release*, 117, 380-386 (2007).
132. Chung Y-I., Ahn K.-Min, Jeon S-H., Lee S-Y., Lee J-H. and Tae G., '*Enhanced bone regeneration with BMP-2 loaded functional nanoparticle-hydrogel complex*', *J. Control. Release*, 121 (1-2), 91-99 (2007).
133. Yuan Y., Chesnutt B.M., Utturkar G., Haggard W.O., Yang Y., Ong J.L. and Bumgardner J.D., '*The effect of cross-linking of chitosan microspheres with genipin on protein release*', *Carbohydrate Polymers*, 68 (3), 561-567 (2007).
134. Al-Kassas R. S., Al-Gohary O. M.N. and Al-Faadhel M. M., '*Controlling of systemic absorption of gliclazide through incorporation into alginate beads*', *Intern. J. Pharma*, 341 (1-2), 230-237 (2007).
135. George M. and Abraham T. E., '*Polyionic hydrocolloids for the intestinal delivery of protein drugs: Alginate and chitosan*', *J. Control. Release*, 114 (1), 1-14 (2006).
136. Liu L. S., Liu S. Q., Ng S. Y., Froix M., Ohno T. and Heller J., '*Control. release of interleukin-2 for tumor immunotherapy using alginate/chitosan porous microspheres*' , *J. Control. Release*, 43, 65-74 (1997).
137. Cui F., Cun D., Tao A., Yang M., Shi K., Zhao M. and Guan Y., '*Preparation and characterization of melittin-loaded poly (dl-lactic acid) or poly (dl-lactic-co-glycolic acid) microspheres made by the double emulsion method*', *J. Control. Release*, 107 (2), 310-319 (2005).

138. Chen L. and Subirade M., '*Effect of preparation conditions on the nutrient release properties of alginate-whey protein granular microspheres*' *Europ. J. Pharma. Biopharma.*, 65 (3), 354-362 (2007).
139. Kulkarni A. R., Soppimath K. S. and Aminabhavi T. M., '*Controlled release of diclofenac sodium from sodium alginate beads crosslinked with glutaraldehyde*', *Pharmaceutica Acta Helvetiae*, 74 (1), 29-36 (1999).
140. Xu Y., Zhan C., Fan L., Wang L. and Zheng H., '*Preparation of dual crosslinked alginate-chitosan blend gel beads and in vitro controlled release in oral site-specific drug delivery system*', *Intern. J. Pharma.*, 336 (2), 329-337 (2007).
141. Hari P.R., Chandy T. and Sharma C.P., '*Chitosan/calcium-alginate beads for oral delivery of insulin*', *J. Appl. Polym. Sci.* 59, 1795-1801 (1996).
142. Arica B., Çalı S., Ka H. S., Sargon M. F. and Hıncal A. A., '*Fluorouracil encapsulated alginate beads for the treatment of breast cancer*', *Intern. J. Pharma.*, 242 (1-2), 267-269 (2002).
143. Hejazi R. and Amiji M., '*Stomach-specific anti-H. pylori therapy. I: preparation and characterization of tetracycline-loaded chitosan microspheres*', *Intern. J. Pharma.*, 235 (1-2), 87-94 (2002).
144. Smidsrod O., '*The relative extension of alginates having different chemical composition*', *Carbohydr. Res.* 27, 107-118 (1973).
145. Van Tomme S. R., De Geest B. G., Braeckmans K., De Smedt S. C., Siepmann F., Siepmann J., van Nostrum C. F. and Hennink W. E., '*Mobility of model proteins in hydrogels composed of oppositely charged dextran microspheres studied by protein release and fluorescence recovery after photobleaching*', *J. Control. Release*, 110 (1), 67-78 (2005).

146. Cooper C.L., Dubin P.L., Kayitmazer A.B. and Turksen S., '*Polyelectrolyte-protein complexes*', *Curr. Opin. Colloid Interface Sci.*, 10, 52 - 78 (2005).
147. Krishnamachari Y., Madan P. and Lin S., '*Development of pH- and time-dependent oral microparticles to optimize budesonide delivery to ileum and colon*', *Intern. J. Pharma.*, 338 (1-2), 238-247 (2007).
148. Gan Q. and Wanga T., '*Chitosan nanoparticle as protein delivery carrier-Systematic examination of fabrication conditions for efficient loading and release*', *Colloids Surface B: Biointerfaces*, 59 (1), 24-34 (2007).
149. Vandenberg G. W., Drolet C., Scott S. L. and J. de la Noüe J., '*Factors affecting protein release from alginate-chitosan coacervate microcapsules during production and gastric/intestinal simulation*', *J. Control. Release*, 77 (3), 297-307 (2001).
150. Almeida P. F. and Almeida A. J. '*Cross-linked alginate-gelatine beads: a new matrix for controlled release of pindolol*', *J. Control. Release*, 97 (3), 431-439 (2004).
151. Silva C. M., Ribeiro A. J., Figueiredo I. V., Gonçalves A. R. and Veiga F., '*Alginate microspheres prepared by internal gelation: Development and effect on insulin stability*', *Intern. J. Pharma.*, 311 (1-2), 1-10 (2006).
152. Stein G. S and Lian J.B., '*Molecular mechanisms mediating proliferation/differentiation interrelationships during progressive development of osteoblast phenotype*', *Endocrine Reviews*, 14 (4), 424-441 (1993).

APPENDIX A

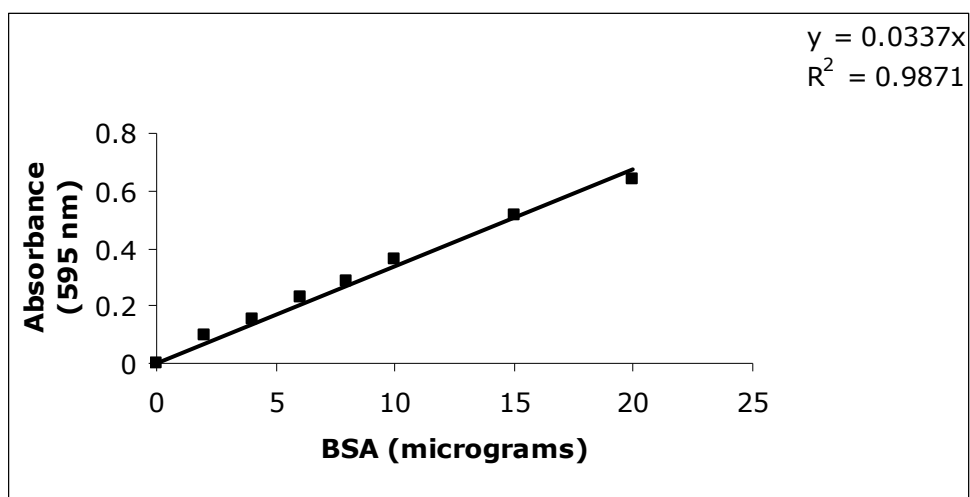


Figure A-1. BSA calibration curve prepared with microBradford assay for encapsulation efficiency study.

APPENDIX B

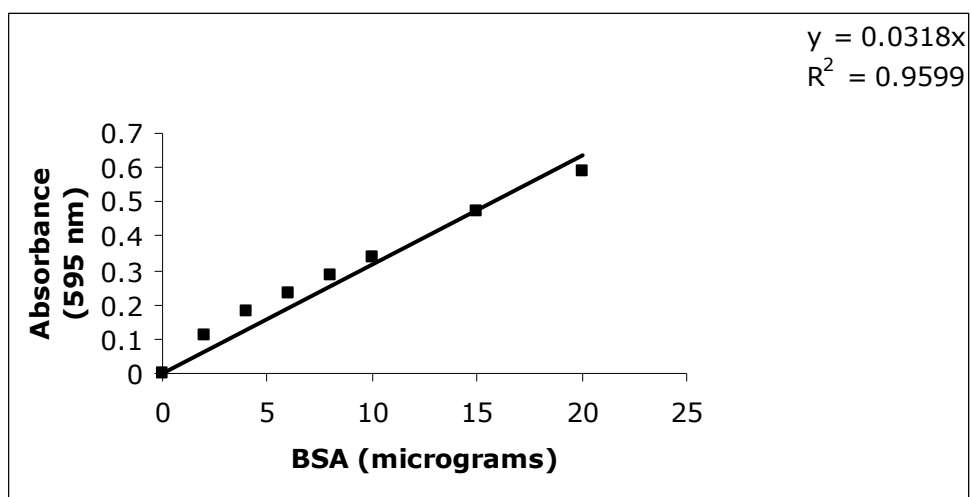


Figure B-1. BSA calibration curve prepared with microBradford assay for release study.

APPENDIX C

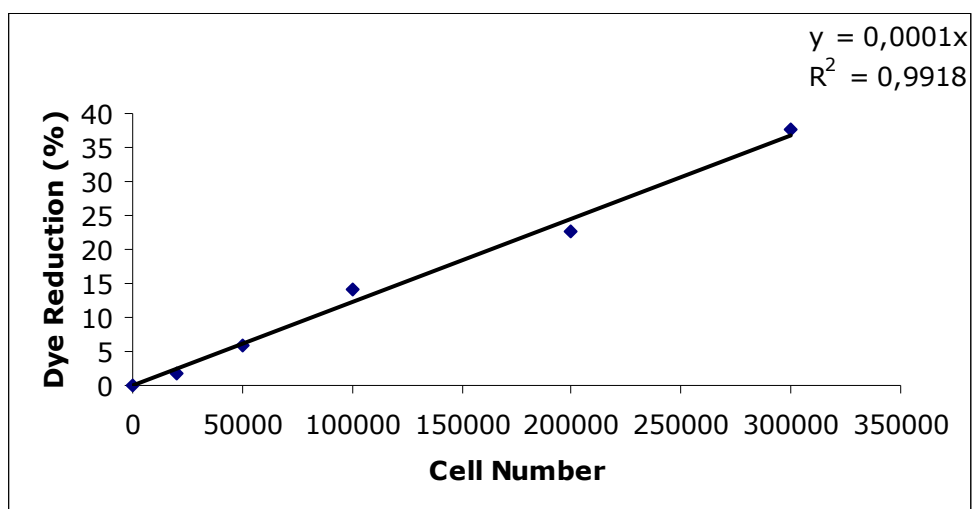


Figure C-1. Calibration curve for BMSCs prepared by Alamar Blue Assay.

APPENDIX D

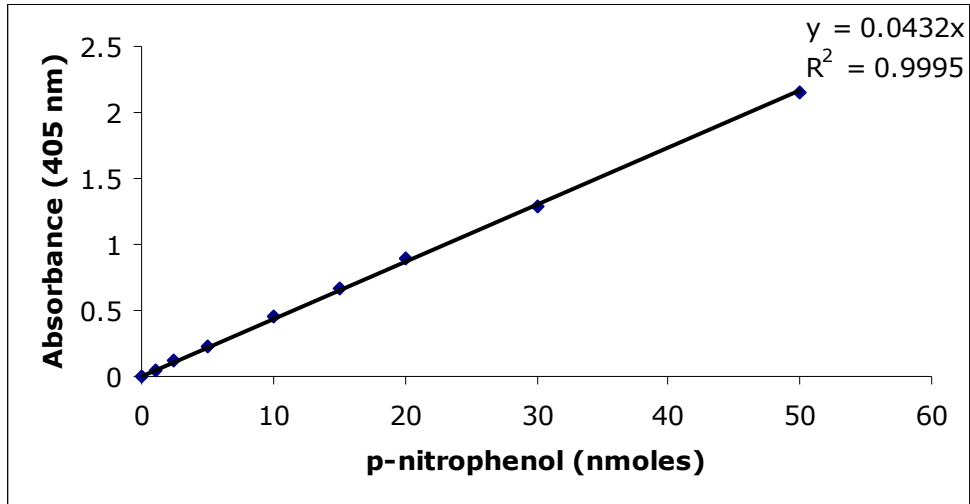


Figure D-1. ALP calibration curve prepared with p-nitrophenol.